

ARCTIC INSTITUTE OF NORTH AMERICA

TECHNICAL PAPER NO. 20

**GEOPHYSICAL MEASUREMENTS ON THE
KASKAWULSH AND HUBBARD GLACIERS,
YUKON TERRITORY**

By

GARRY K. C. CLARKE



PUBLISHED SEPTEMBER 1967

THE ARCTIC INSTITUTE OF NORTH AMERICA

The Arctic Institute of North America was formed to further the scientific study and exploration of the Arctic. The Institute provides information on the Arctic through its three Offices, awards research grants, and publishes scientific papers and other contributions in its journal *Arctic* and other publications. Those interested in this work are invited to become Associate Members. Associates receive all numbers of the journal. The Library and Map Collection at the Montreal Office are principally for their use, and they are welcome there and at the other Institute Offices. Membership dues are \$5.00 annually. All remittances should be sent to the Montreal Office.

Board of Governors

TREVOR LLOYD, (<i>Chairman</i>), Montreal, P.Q.	WILLIAM M. GILCHRIST, Ottawa, Ont. LAURENCE M. GOULD, Tucson, Ariz.
W. S. BENNINGHOFF, (<i>Vice-Chairman</i>), Ann Arbor, Mich.	ERIC GOURDEAU, Quebec, P.Q. GEORGE GRYC, Meno Park, Calif.
DAVID C. NUTT, (<i>Secretary</i>), Hanover, N.H.	LOUIS-EDMOND HAMELIN, Quebec, P.Q.
GEORGE JACOBSEN, (<i>Treasurer</i>), Montreal, P.Q.	CARYL P. HASKINS, Washington, D.C. LAURENCE IRVING, College, Alaska
C. EARL ALBRECHT, Philadelphia, Pa.	HELGE E. LARSEN, Copenhagen, Denmark
COLIN B. B. BULL, Columbus, Ohio	J. ROSS MACKAY, Vancouver, B.C.
JOHN S. DICKEY, Hanover, N.H.	RICHARD H. NOLTE, New York, N.Y.
M. J. DUNBAR, Montreal, P.Q.	SVENN ORVIG, Montreal, P.Q.
MOIRA DUNBAR, Ottawa, Ont.	E. F. ROOTS, Ottawa, Ont.
JOSEPH O. FLETCHER, Santa Monica, Calif.	DIANA M. R. ROWLEY, Ottawa, Ont. I. NORMAN SMITH, Ottawa, Ont.

Executive Director

JOHN C. REED
Washington

Directors of Offices

Washington
R. C. FAYLOR

Montreal
H. W. LOVE

Editor *Technical Series*
DIANA ROWLEY

Editor *Arctic*
ANNA MONSON

Offices of the Institute

3458 Redpath Street, Montreal 25, P.Q., Canada
1619 New Hampshire Avenue, N.W., Washington, D.C. 20009, U.S.A.
46 East 70th Street, New York, N.Y. 10021, U.S.A.

ARCTIC INSTITUTE OF NORTH AMERICA

TECHNICAL PAPER NO. 20

GEOPHYSICAL MEASUREMENTS ON THE
KASKAWULSH AND HUBBARD GLACIERS,
YUKON TERRITORY

By

GARRY K. C. CLARKE



PUBLISHED SEPTEMBER 1967

CONTENTS

Abstract	5
Introduction	5
Reduction and interpretation of gravity measurements	8
Gravity measurements	8
Drift, misclosure, and gravity corrections	9
Determination of ice thickness from gravity measurements	14
Seismic measurements	15
Field work	15
Seismology on glaciers	16
Application of refraction results to reflection seismic results	19
Determination of the depth and spatial orientation of a dipping plane from primary and multiple reflections	19
Results of seismic survey	25
Investigations of glacier flow	28
Measurements of surface flow on the Kaskawulsh and Hubbard glaciers	28
The relationship of surface flow to ice thickness measurements	28
Summary and conclusions	32
Acknowledgments	35
References	35

Tables

1. Weights and corrections for gravity differences	10
2. Results of seismic refraction measurements	17
3. Velocities of P waves in glacier ice	18
4. Filter data	21
5. Annual movements of flow stakes	29

Figures

1. Photomosaic of a divide between the Kaskawulsh and Hubbard glaciers	4
2. Location of metal flow stakes and seismic stakes from Survey II, 1963, by D. Sharni <i>folding map</i>	
3. Schematic diagram of gravity network and misclosures	9
4. Bouguer anomaly profiles	12
5. Refraction arrival times	16
6. Velocity of P waves with depth	17
7. Curved ray paths in the firn layer	18
8. Coordinates of detectors, shot point, and image shot point	20
9. Correction for shot depth	20
10. Spatial orientation of the plane of the three detectors	20
11. Multiple reflections from a dipping plane	23
12. Bedrock profiles from geophysical measurements	26
13. Bedrock topography and surface flow rates	30, 31
14. Seismic records	33, 34

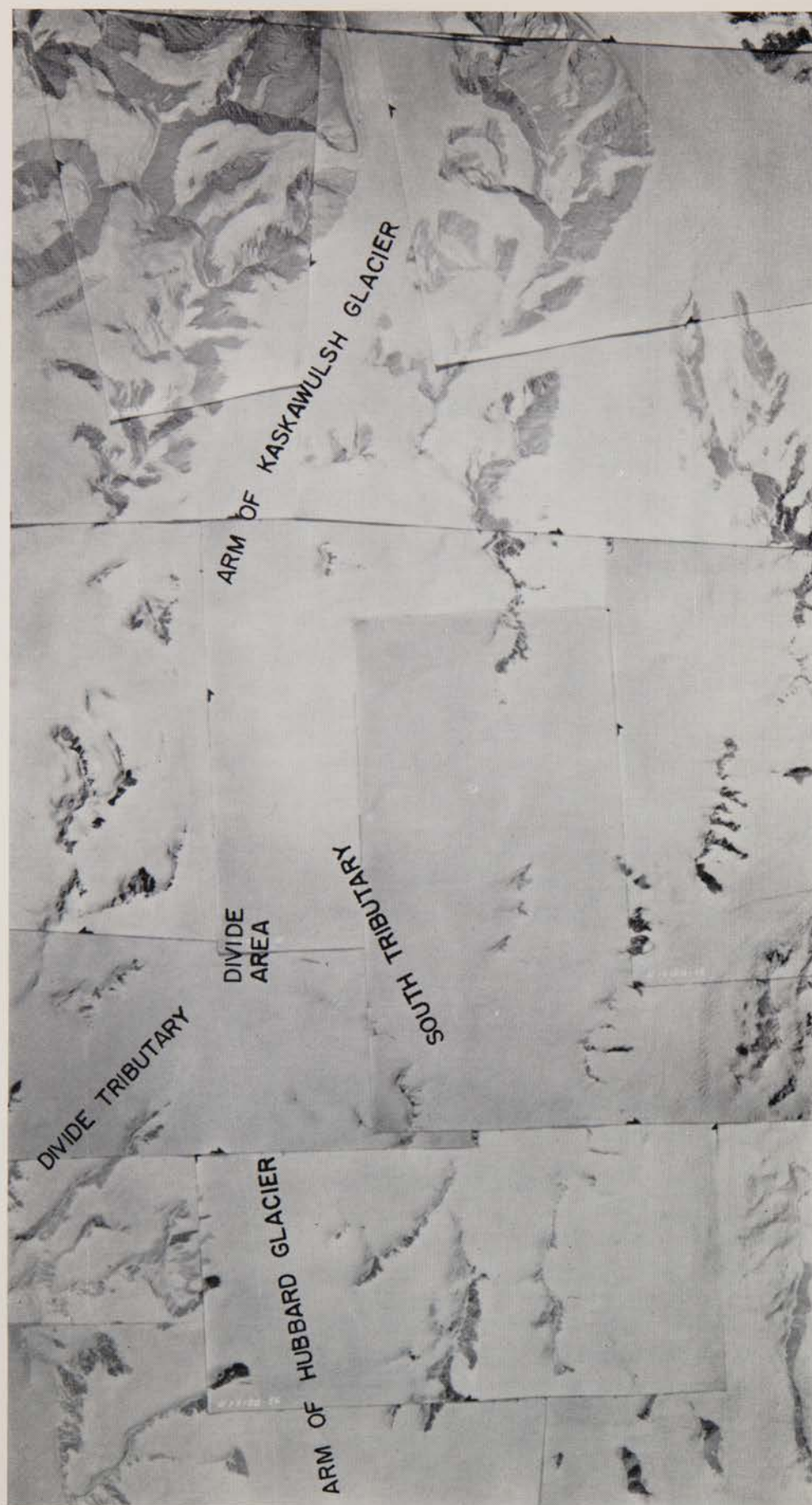


Fig. 1. Photomosaic of a divide between the Kaskawulsh and Hubbard glaciers.

GEOPHYSICAL MEASUREMENTS ON THE KASKAWULSH AND HUBBARD GLACIERS, YUKON TERRITORY

Garry K. C. Clarke¹

Abstract

Gravity and seismic measurements made in the summer of 1963 were used to determine ice thickness in the divide region of the Kaskawulsh and Hubbard glaciers (60° 45N, 139° 40W) in the St. Elias Mountains of the Yukon Territory, Canada. Gravity differences were measured for a network of 107 gravity stations and Bouguer anomalies ranged from -199.8 mgal to -162.9 mgal. Crude ice-thickness calculations were made from these results assuming the glacier was an infinite slab. Seismic refraction lines on the Kaskawulsh and Hubbard glaciers gave a firm thickness of approximately 40 m and an average P-wave velocity of 3710 ± 20 m/sec. One hundred seismic reflection stations were occupied and, discounting poor results, the maximum ice thicknesses found were 778 m at stake 1 on the Kaskawulsh Glacier and 539 m at stake 29 on the Hubbard Glacier. The maximum surface flow rates measured were 150 m/yr at stake 1 on the Kaskawulsh Glacier and 132 m/yr at stake 44 on the Hubbard. A close relationship was found between geophysically-determined ice thicknesses and surface flow measurements. The flow line and the line of the valley centre proved to be roughly coincident, although flow was complicated by tributary glaciers. The topographic divide was also the flow divide but no corresponding bedrock divide was found.

Introduction

The development of mathematical theories of glacier flow has emphasized the necessity of knowing the cross-sectional shape of glaciers as a starting point for applying flow theory. At present geophysical methods provide the most practical approach to the problem of finding the dimensions of a glacier. For this reason the Icefield Ranges Research Project has supported seismic and gravity measurements which provide independent and complementary methods of calculating ice thickness and hence of mapping the underlying bedrock surface. This paper describes geophysical work in 1962 and 1963 in the vicinity of the divide between tributaries of the Kaskawulsh and Hubbard glaciers in the St. Elias Mountains of the Yukon Territory.

The Icefield Ranges Research Project (IRRP), a joint undertaking of the Arctic Institute of North America and the American Geographical Society, is directed by Dr. W. A. Wood with Mr. R. H. Ragle as field leader. The first reconnaissance took place in the summer of 1961 and field work has continued

¹Department of Physics, University of Toronto.

each succeeding summer. Since the project aims to study the total mountain environment, scientists from the disciplines of glaciology, geology, geophysics, and meteorology are participating.

The St. Elias Mountains, which lie between the Western Yukon Plateau and the Pacific Ocean, are the highest mountains of Canada. With the ranges of the Vancouver, Queen Charlotte, and the southeastern Alaskan coast islands, the St. Elias Range forms the Outer Mountain area of the Canadian Cordillera (Bostock, 1948). In Canada the range covers approximately 320 km by 150 km in southwestern Yukon and northwestern British Columbia. The extensively glacierized central region is known as the Icefield Ranges; from this accumulation area at an elevation of over 2100 m drain five of the world's longest valley glaciers outside the polar regions: the Hubbard, Walsh, Donjek, Kluane, and Kaskawulsh glaciers (Wood, 1963). The common accumulation area of these glaciers forms a highland glacier as defined by Ahlmann (1933). Near latitude $60^{\circ}45'N$ and $139^{\circ}40'W$, fifty kilometres north of the International Boundary with Alaska, a divide at 2636 m separates tributary glaciers of the Kaskawulsh and Hubbard systems (Fig. 1) and it was this area which was studied in 1962 and 1963. To the east flows the North Arm of the Kaskawulsh Glacier, joining with the Main and South arms to form a valley glacier over 70 km long, with its terminus at the headwaters of the Slims and Kaskawulsh rivers which flow into the Yukon and Alsek drainage systems respectively. The Hubbard Glacier which is 120 km long flows southward to Disenchantment Bay in the Gulf of Alaska.

The Icefield Ranges are the largest group of great peaks in North America; most of these peaks are in Canada or along the Alaska-Yukon Boundary. Within a 50-km radius of the Kaskawulsh-Hubbard Divide stand the Logan Massif (6050 m), Mt. Vancouver (4785 m), Mt. Lucania (5227 m), Mt. Steele (5011 m), Mt. Alverstone (4420 m), and Mt. Hubbard (4557 m).

In 1951 the St. Elias Mountains between Kluane Lake and the Alaska border were photographed through an R.C.A.F. contract. Subsequently (1962) the Canadian Government published the Mount St. Elias Map Sheet (Mt. St. Elias 115B and 115C, 1:250,000) based on the photogrammetric survey and using control points established during the International Boundary Survey.

In 1961 a theodolite survey by R. W. Mason and W. A. Wood of the Icefield Ranges Research Project established a network of known points, one triangulation station of which was tied by resection to six points of the 1913 International Boundary Commission Survey. Based on the surface work of Mason and Wood and the Canadian photographs the Ohio State University Research Foundation prepared a map of the divide area being studied by the Icefield Ranges Project, on a 1:25,000 scale which was reproduced by the American Geographical Society (Wood, 1963) on a scale of 1:30,000. The Ohio State University map was used as the base map for the geophysical work (Fig. 2).

Some 60 metal flow stakes were set up and surveyed by theodolite in 1962 to determine location and elevation. The following year these stakes were surveyed at the beginning and the end of the summer season by Dan Sharni to determine annual and summer flow rates and changes in surface elevation; in this paper the surveys by Sharni are referred to as Survey I and Survey II respectively. Horizontal coordinates and elevations of special geophysical

marker stakes were also surveyed by Sharni in 1963 and are referred to as the Seismic Survey.

In 1963 scientific work from the Glacier Camp (see Fig. 2) consisted of meteorological observations, glaciological studies, geophysical measurements to determine ice thickness, and the above-mentioned theodolite surveys. Meteorological studies were centred at a camp near the divide at elevation 2641 m (Havens and Saarela, 1964) with other observations being made from Base Camp, Glacier Camp, and Kaskawulsh Camp at the terminus of the Kaskawulsh Glacier (Ragle, 1964). Glaciological investigations have so far included stratigraphic studies, surface flow measurements, and determination of oxygen isotope abundances. Preliminary studies by Ragle, confirmed by temperature measurements (Wagner, personal communication) would indicate that at 2600 m the glacier is sub-polar by both Ahlmann's geophysical classification (Ahlmann, 1933) and Benson's facies classification (Benson, 1962).

Geophysical studies on the project were initiated by A. Becker in 1962. A high-quality seismic refraction profile was obtained, 14 reflection stations were occupied, and gravity was measured at the metal flow stakes. The following summer geophysical studies were continued by the writer; it is the results of these measurements which form the bulk of this paper. Seismic work during the summer of 1963 consisted of a refraction profile to obtain velocity-depth relations and hence the thickness of the firn layer and the velocity of P waves in the glacier ice, as well as reflection seismic measurements to find the thickness of the glacier and the orientation in space of the reflecting surfaces. A gravity survey was also made, but since the seismic method is considerably more accurate and direct, it was decided to use the gravity results merely to support the seismic results, to check for multiple reflections, and when necessary to interpolate between high-quality-reflection stations.

REDUCTION AND INTERPRETATION OF GRAVITY MEASUREMENTS

Gravity measurements

Gravimetric surveys of glaciers have a number of attractive features: they are rapid and inexpensive; the gravimeter is light and portable—a significant factor in difficult terrain, and owing to the high density contrast between ice and rock the anomalies are pronounced. The difficulties to be faced are the severity of climatic conditions, requiring a high degree of temperature stability in the gravimeter, and the roughness of transportation necessitating a rugged instrument. On mountain glaciers the terrain corrections are often large, and if much of the region is ice-covered it may be difficult to estimate these corrections very accurately; moreover in mountainous regions structural trends may give rise to gravity gradients.

A Worden gravimeter was used for the entire 1963 survey. This instrument has a zero-length quartz spring and a thermal compensating spring with the entire system mounted in a vacuum flask to reduce temperature effects (Heiskanen and Meinesz, 1958). The particular Worden gravimeter used, Instrument XPO, had a small-range (185 mgal) dial and a reset screw but not a geodetic dial for long-range measurements. The instrument was calibrated by measuring the gravity difference between the University of Wisconsin Geodetic Station in the Geophysics Laboratory (Rm. 18) of the Physics Building of the University of Alberta at which $g = 981.1695$ gals and the Dominion Observatory pendulum station in the basement of the Federal Building in Red Deer at which $g = 980.9988$ gals (Garland and Tanner, 1957). The Edmonton station was occupied three times and the Red Deer station twice to form an ABABA loop with five readings taken each time. The resulting scale constant was found to be $0.2352(8)$ mgals/division with a standard deviation of 0.00005 mgals/division compared with the factory-calibrated value of $0.2354(7)$ mgals/division.

Placing the gravimeter tripod on a sturdy wooden sled proved a satisfactory method of stabilizing the instrument although in a brisk wind the sled tended to vibrate. Unfortunately the particular Worden gravimeter used was highly sensitive to changes in temperature so that many loops had to be repeated to obtain reasonable closure. Loops for which there were readings giving a deviation of more than one scale division from a linear drift line were rejected and the loop was repeated. Stable weather conditions with a light breeze proved ideal for gravity surveying. Repeated measurements between rock stations (at the triangulation cairns) and glacier stations (at the marker stakes) were often poorly duplicated and it is supposed that this was due to their differing temperature conditions. Even when agreement was satisfactory it did not necessarily imply that the actual measurement of the gravity difference was correct owing to the contrasting environments of the two stations. Such an error would appear as poor closure about a loop.

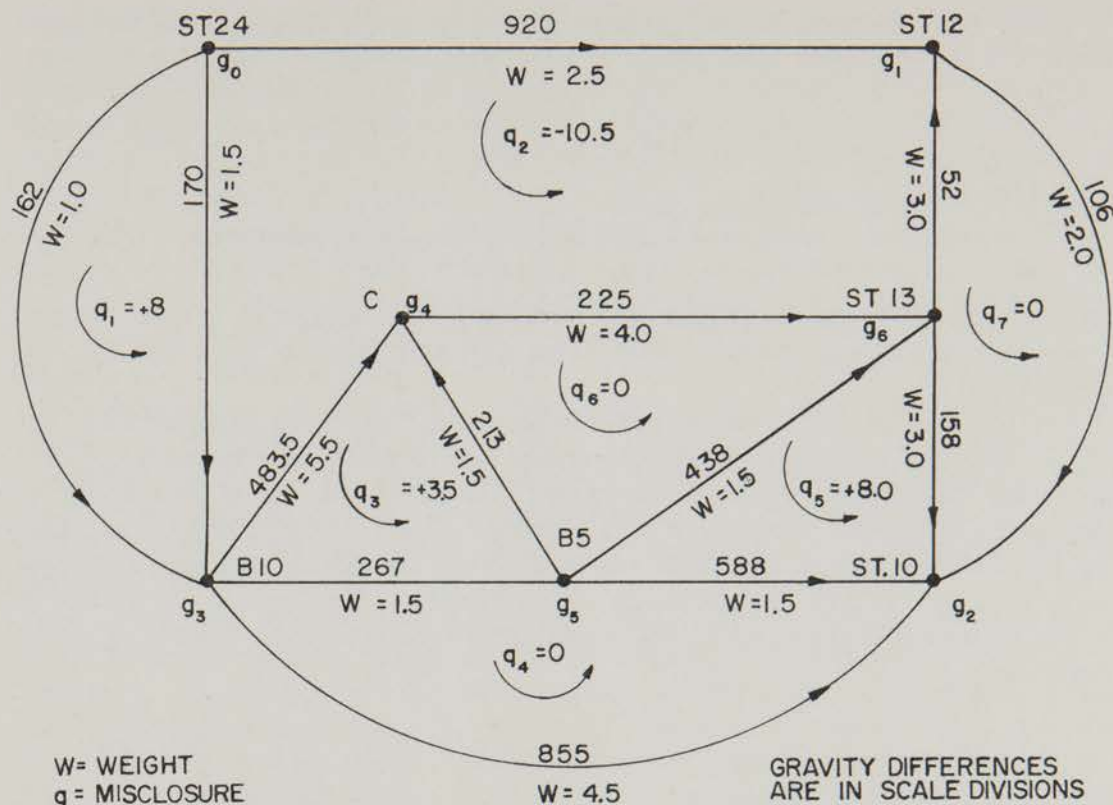


Fig. 3. Schematic diagram of gravity network and misclosures.

Drift, misclosure, and gravity corrections

Corrections for drift and misclosure were first applied to the raw field measurements to make the data self-consistent. The corrected field values were then converted to gravity units and corrections applied to make each station directly comparable. Such corrections included corrections for latitude, elevation, and terrain and for geology and isostasy if required.

The drift measured by a spring gravimeter is the sum of the tidal or actual drifts and instrument drifts resulting from relaxation of components and thermal effects on components. The tidal drift is of small amplitude and is a smooth sinusoidal-like function. The drift due to relaxation is small and always positive seldom exceeding 0.03 mgal/hr. The thermal drift is minimized by a compensating spring which counteracts length changes in the main spring. Mounting in a vacuum flask further reduces thermal effects. Some systems have a thermostatic heating element which maintains the temperature of the gravimeter at a constant temperature. Ideally thermal drifts can be kept very low, however, the particular instrument used had high and erratic drift suggesting that the gravimeter had lost its vacuum.

The method of looping was used to establish legs of the gravity traverse, a typical sequence of stations being of the form ABABCDEF A. The network of gravity stations consisted of seven large loops allowing the closure of the survey to be checked. Because each measurement of gravity is subject to a small random error, misclosures resulted which were subsequently adjusted by means of a least squares method (Gibson, 1941). The seven loops, the measured gravity differences and misclosures are represented schematically in Fig. 3.

Weights were assigned to each branch of the network according to the parameter

$$w = \sqrt{\frac{100n}{t(1+\Delta)}}$$

where n = number of readings at a station

t = average time in minutes required to travel between two end stations

Δ = maximum difference in readings at a station

which proved to give a satisfactory distribution of weights. These weights were normalized and rounded off. The adjusted solution must satisfy two conditions:

(1) the sum of the corrected differences around any loop must be zero,

(2) the sum of the weighted corrections at any node must be zero,

these are directly analogous to Kirchhoff's circuit laws. It is convenient to define the reciprocal weight as the "adjustability", $a = 1/w$. The desired least squares solution minimizes $\sum k_i^2 a_i$ where k_i is the correction to a particular observation, just as $\sum i^2 r$ is a minimum for circuitry. The option of a loop or nodal approach is presented. The nodal approach yields the following set of equations:

$$\begin{Bmatrix} +3.5 & -2.5 & 0 & -2.5 & 0 & 0 & 0 \\ -2.5 & +7.5 & -2.0 & 0 & 0 & 0 & -3.0 \\ 0 & -2.0 & +11.0 & -4.5 & 0 & -1.5 & -3.0 \\ -2.5 & 0 & -4.5 & +14.0 & -5.5 & -1.5 & 0 \\ 0 & 0 & 0 & -5.5 & +11.0 & -1.5 & -4.0 \\ 0 & 0 & -1.5 & -1.5 & -1.5 & +6.0 & -1.5 \\ 0 & -3.0 & -3.0 & 0 & -4.0 & -1.5 & +11.5 \end{Bmatrix} \begin{Bmatrix} g_0 \\ g_1 \\ g_2 \\ g_3 \\ g_4 \\ g_5 \\ g_6 \end{Bmatrix} = \begin{Bmatrix} +2717.0 \\ +2356.0 \\ -5415.5 \\ +6490.3 \\ -2078.8 \\ +1958.0 \\ -927.0 \end{Bmatrix}$$

This set of equations was solved by the University of Toronto's 7090 Computer. The resulting adjustments are summarized in Table 1.

Table 1. Weights and corrections for gravity differences.

<i>Observation</i>	<i>Weight</i>	<i>Difference observed (scale divisions)</i>	<i>Calculated difference</i>	<i>Observed— Calculated</i>
St.24-St.12	2.5	920.0	920.2	-0.2
St.24-G-St.B10	1.0	162.0	166.6	-4.6
St.24-St.B10	1.5	170.0	166.6	+3.4
St.12-St.13	3.0	52.0	50.4	+1.6
St.13-St.10	3.0	158.0	154.4	+3.6
St.12-St.10	2.0	106.0	104.0	+2.0
St.B10-St.10	4.5	855.0	857.6	-2.6
St.B10-C	5.5	483.5	481.1	+2.4
St.B10-St.B5	1.5	267.0	267.5	-0.5
St.B5-St.10	1.5	588.0	590.1	-2.1
St.B5-St.13	1.5	438.0	435.7	+2.3
St.13-C	4.0	225.0	222.1	+2.9
St.B5-C	1.5	213.0	213.6	-0.6

A latitude correction must be applied to measured gravity values to eliminate the combined effects of the earth's rotation and ellipticity of the earth. The 1930 International Gravity Formula defines the theoretical value of gravity for a station located at sea-level as $\gamma = (978.0490) (1 + 0.0052884 \sin^2 \phi - 0.0000059 \sin^2 2\phi)$ gals where ϕ is the latitude of the station. Referring all stations to cairn B at latitude $\phi = 60^\circ 45'N$ and assuming the map grid to be spherical the correction for a station a distance y metres north of the reference station is -0.0006938 mgal/metre.

A free air correction must be applied to reduce all gravity measurements to the same datum elevation (usually sea-level or the geoid). The expression $\partial g / \partial r = -0.30855 - 0.00022 \cos 2\phi + 0.000144 h$ mgal/m takes into account the variation in this correction with latitude (Garland, 1956) so that for a latitude $\phi = 60^\circ 45'$ and altitude $h = 2.636$ km the free air correction is -0.30804 mgal/m. To compensate for material between the gravity station and the datum plane the Bouguer correction $g_b = 2\pi k \rho h$ must be added where k is the gravitational constant and ρ is the density of the slab material (Heiskanen and Meinesz, 1958). In the following gravity analysis the glacier ice is taken to be the anomalous material replacing rock. To evaluate the regional density, representative rock samples are usually collected and their densities measured. In the Icefield Ranges outcrops are sparse and often quite inaccessible. Although rock samples were collected at those triangulation cairns at which gravity was measured it was decided that these samples could in no way be considered representative. The cairns were situated on resistant outcrops, and the very fact that they had not been eroded away by the glacier would suggest that they were not typical of the local geology and possibly of a higher density than the true regional density. Rather than propose a regional density from such a small number of rock samples it was decided to accept $\rho = 2.67$ gm/cm³ as the regional density so that the Bouguer correction was 0.1119 mgal/m. Hence the complete elevation correction, that is Bouguer correction plus free air correction, was -0.1961 mgal/m.

Since in general the material between the gravity station and the datum plane is not an infinite slab, a further correction must be applied to compensate for variations from the slab, that is, topographic irregularities. This terrain correction is always positive, since any deviation from a slab tends to reduce gravity. If the topographic irregularities are effectively of infinite extent in one dimension then simple two-dimensional corrections may be applied (Hubbert, 1948 a, b) using charts or a line-integral method. Unfortunately this situation is not encountered in the area studied. Because of its simplicity the Hammer system of zones (Nettleton, 1940) was used to estimate terrain corrections although this method is not well adapted to the prevailing conditions. First the available maps are not entirely satisfactory for this purpose, also the Hammer method assumes that terrain effects are due to a single material of constant density whereas in the glacier region there are two materials of widely differing densities, ice and rock. A further difficulty in estimating terrain corrections is that the thickness of the widespread glacier cover is not well known; in some areas there is only a thin cover above the rock and in others deep tributary glaciers join the main glacial channel.

Since the two area maps available are the Ohio State University map (1:25,000) of the immediate study area and the Department of Mines and Technical Surveys map (1:250,000) it was decided to divide the terrain correction

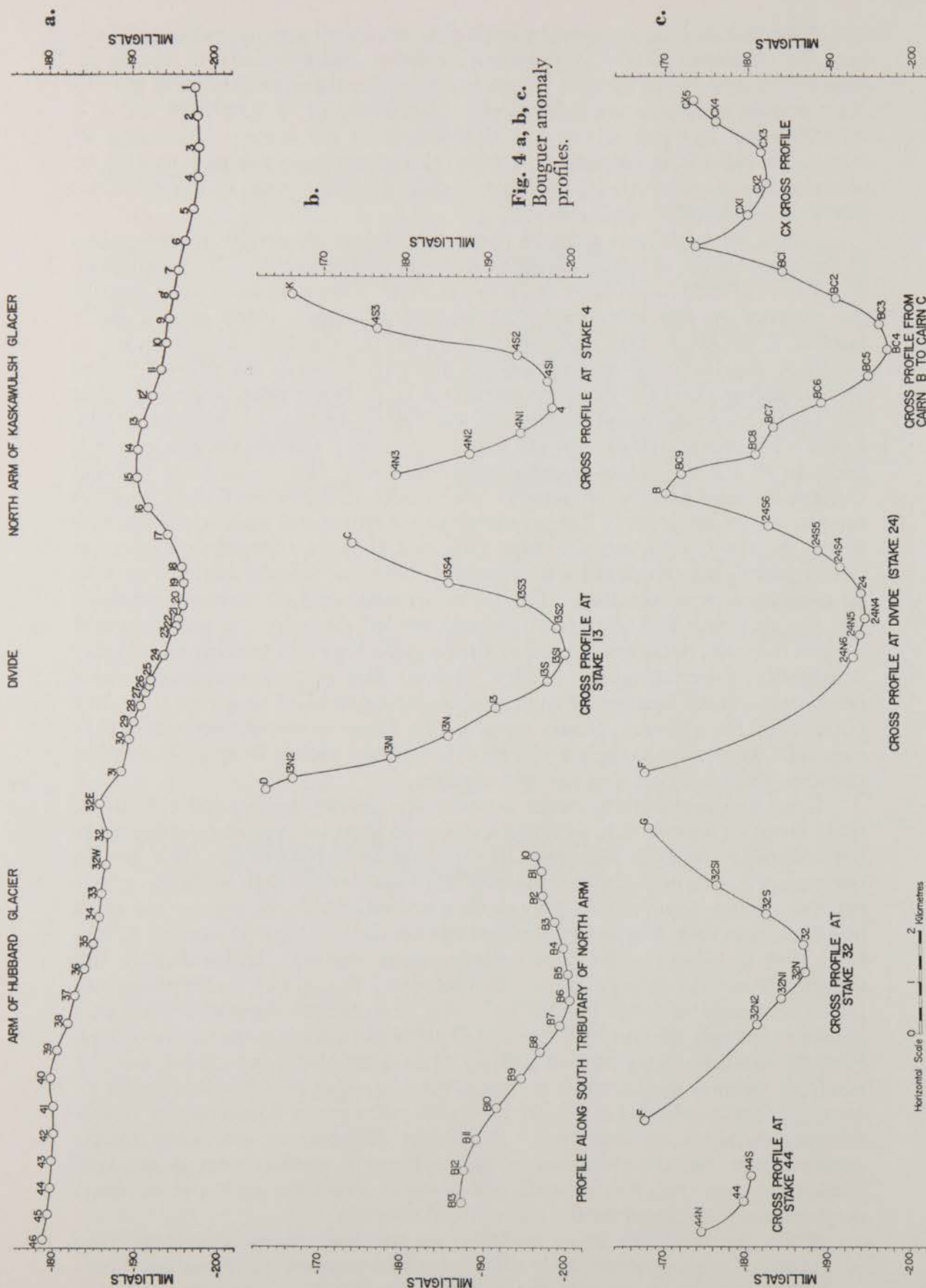


Fig. 4 a, b, c.
Bouguer anomaly
profiles.

into two parts: a near-correction including terrain effects within 4470 m of the gravity station determined from the 1:25,000 map, and a far-correction for effects between a 4470- and 21,940-m radius of the station determined from the 1:250,000 map. No correction was made for terrain beyond this outer radius because the effect of this was fairly constant for the entire network of stations. In the near-correction no consideration was given to regions below the station elevation for glacier stations because this was the anomaly being sought. All terrain above the station elevation and not in the main glacier channel was considered to have a density of 2.67 gm/cm^3 . No correction was made for areas of the main glacier above the station elevation since this correction was negligible. For the cairn stations the near-correction included a correction for the voids between the station and the elevation of the glacier surface but not for material below this elevation. The far-correction considered terrain effects below the station elevation as well as above.

The value of the far-correction was computed at 14 representative locations and varied from 0.41 to 0.88 mgals. Values at intermediate stations were obtained by contouring the values of the control stations. The near-correction was computed at 47 stations and these results were also contoured to give values at the remainder of the stations. The terrain correction is extremely sensitive to terrain effects very near the station, and without detailed mapping at the station site becomes highly uncertain. This presented no problem for the glacier stations since there were no near-terrain effects. The cairn stations, on the other hand, were often perched on rock pinnacles and hence the near-terrain effects were very large and very uncertain. Little faith can therefore be placed in the values of the Bouguer anomaly for cairn stations and thus a regional trend cannot be established from the cairn stations.

Two additional factors could be considered which are peculiar to gravity measurements on glaciers. First, a glacier is in constant motion so that the surveyed values of the coordinates are not the values of the actual station if there is a time lapse between the survey and the gravity measurement. Secondly, the surface of the glacier changes as a result of ablation and accumulation. Because the maximum interval between the second survey and the gravity measurement was only 27 days, and the maximum annual flow was 150 metres no correction for motion was considered necessary. Daily measurements of the changes in the elevation of the snow surface at the divide show the maximum change over the 25-day interval from July 26 to August 19, during which gravity measurements were taken, to be 21.5 cm (Havens, personal communication). Errors resulting from surface lowering are mainly due to differential melting between stations; as such errors are not large and are distributed throughout the entire network it was decided to neglect any correction. Hence the snow surface elevations computed by Sharni for Survey I and the Seismic Survey and the coordinates from Survey II and the Seismic Survey are used throughout.

Owing to the small range of the gravimeter and the shortage of aircraft time, it was not possible to tie the network of gravity sections to a geodetic station in 1963. However in 1962 Becker (personal communication) measured the gravity difference between stake 16 and the Dominion Observatory station at Kluane Village on the Alaska Highway (Oldham, 1958). No permanent gravity station was established in the region of the glacier at that time to which subsequent gravity measurements could have been tied. However the 1963

survey results show that stake 24 near the topographic divide has moved only 8 metres since 1962 (Sharni, 1963) and the elevation of the snow surface increased by 2.6 metres. Using Becker's gravity difference for $g_{24} - g_{16}$ and allowing for 2.6 metres of firn of density $\rho = 0.5 \text{ gm/cm}^3$, the 1963 value of absolute gravity at stake 24 should be 981,272.4 mgals to within 1.5 mgals. For the other stations the gravity differences are probably correct to ± 0.5 mgals, and these are referred to the value at stake 24.

Determination of ice thickness from gravity measurements

Before selecting an interpretation approach for the gravity results, a thorough appraisal of the aims and limitations of the particular gravity survey must be made. The simplest but least accurate approach is to imagine the anomaly is due to an infinite horizontal slab of material. The two-dimensional analysis of Hubbert (1948a) or the three-dimensional analysis of Talwani and Ewing (1960) should give better results. In the region of the Glacier Camp the regional density has not been determined and the regional trends have not been isolated. In most of the study area neither the assumption of an infinitely long two-dimensional glacier nor the assumption of an infinite slab give good approximations. However, good seismic results were obtained at almost all gravity stations. The conclusion is that unknown factors are too great to warrant a very sophisticated interpretation approach, and that the Bouguer anomaly profiles should be used only to assist seismic interpretation. The infinite slab assumption, though not very accurate, is easily handled and provides a basis for comparing the seismic and gravity depths directly. The anomaly due to an infinite slab with density contrast ρ and thickness h is

$$g = 2\pi k\rho h.$$

The Bouguer anomalies, assuming a value of absolute gravity of 981,272.4 mgals at stake 24 and a regional density of 2.67 gm/cm^3 , with all pertinent data for each gravity station are to be found in the writer's thesis (Clarke, 1964). To determine the ice thickness from the Bouguer anomaly it is necessary to know what part of the total anomaly is due to regional effects and what part is due to the glacier ice; this establishes a "zero-line" for the anomaly curve. In the absence of satisfactory stations for establishing regional trends these were assumed to be negligible. The zero-line was taken to make the seismic and gravity bedrock profiles as nearly coincident as possible and the density of glacier ice was assumed to be 0.91 gm/cm^3 for this ice-thickness calculation. The Bouguer anomaly profiles are shown in Fig. 4;¹ the infinite slab ice-thickness profiles are included in Fig. 12. A discussion of the seismic and gravity bedrock profiles is given in the following chapter on seismic results.

¹The Bouguer anomaly profiles in Fig. 4 were plotted assuming the grid of the map to be oriented so that grid north and true north were coincident. It was later learned that grid north is actually 10° from true north and a slight error in the latitude correction results. Since the character of the Bouguer anomaly profile is unchanged by this error Fig. 4 has not been altered.

SEISMIC MEASUREMENTS

Field work

In 1963 a total of 100 reflection stations was occupied with satisfactory results obtained at the majority of these. A refraction profile was also obtained on the Hubbard Glacier. A twelve-channel high-resolution seismograph manufactured by Houston Technical Laboratories (now Texas Instruments) with a recording oscillograph was used for all seismic work. The speed of the recording paper was 20 inches/sec (50.8 cm/sec) with timing lines every 0.005 sec; 500 cps galvanometers were used as output for all ordinary channels and a 200 cps galvanometer for the Log Level Indicator Trace (which was connected to Channel 10). Up to 40 db of initial suppression were used and automatic gain control was in constant operation. Extensive band-pass filtering was adopted with a double section of M-derived low-cut filters and a single section of M-derived high-cut filters. A pass band of 40 cps to 90 cps was typical although the frequency of reflections varied considerably with the depth of the reflecting layer. Velocity type moving-coil seismometers having a natural frequency of 13 cps were used.

A variation of the L-spread was resorted to so that the strike and dip as well as the depth of the reflecting "plane" could be calculated. Unfortunately the 50-foot (15.2-m) detector spacing meant that the lengths of the perpendicular arms of the "L" were too short to give the highly accurate step-out times required for the accurate determination of strikes and dips. Nevertheless it was possible to distinguish oblique reflections from near-vertical ones.

A 60 per cent high-density high-velocity nitroglycerine-type explosive (CIL Geogel) detonated by No. 8 electrical blasting caps (CIL Seismocaps) supplied the source of seismic energy. The firing current was provided by a capacitor-discharge type blaster which gave a sharp time-break pulse which was recorded on trace 13 of the seismic records. Shots were generally buried in the firn layer at a depth of 3–4 m by means of a SIPRE coring auger. At a depth of 3 m explosions did not penetrate the snow surface but a "second shot" phenomenon presumably caused by slumping at the shot point (Figs. 14 a, b) frequently obscured seismic reflections. At a 4-m shot depth this slumping was not recorded and the coupling of seismic energy was appreciably improved. When repeated shots were required to obtain satisfactory reflections at a particular location, the original shot holes were redrilled and the "sprung" hole was used. This proved a very effective means of coupling seismic energy and high-quality reflections were often obtained. A shot size of 2.5 lb (1.13 kg) of high explosives proved satisfactory at most reflection locations while for the refraction line shot size ranged from a single blasting cap to 25 lb of high explosives.

Two seismic refraction profiles have been completed in the region of the Glacier Camp: one in 1962 by Becker near stake 10 on the North Arm of

the Kaskawulsh Glacier, the other in 1963 by the writer near stake 32 on the Hubbard Arm. These were obtained at the beginning and end of the summer ablation period respectively. Neither of these profiles was reversed since it seemed reasonable that the firn-ice contact would closely parallel the snow surface. For this reason elevation corrections were also considered unnecessary as the snow surface was effectively an inclined plane.

Seismology on glaciers

Above the firn line a glacier is seismically two-layered: a homogeneous layer of glacier ice, density $0.88\text{--}0.91\text{ gm/cm}^3$, and an overlying firn layer, with density increasing from as low as 0.4 gm/cm^3 at the surface (Bader *et al.*, 1954) to that of glacier ice at the lower boundary. Seismic refraction enables the determination of the velocity distribution of P waves in the glacier. It has been observed that the hexagonal ice crystals often take on a preferred orientation in which the "c" axis (the slow axis) is near vertical or perpendicular to the maximum shear plane so that the medium is classified as transversely isotropic since it possesses a symmetry axis. Such a medium has five elastic constants not two as does the isotropic solid (Love, 1944). The anisotropy is not usually strong enough to affect seriously the refraction results. By means of perpendicular refraction lines and uphole shots Paterson and Savage (1963) showed that there was no significant anisotropy on the Athabasca Glacier.

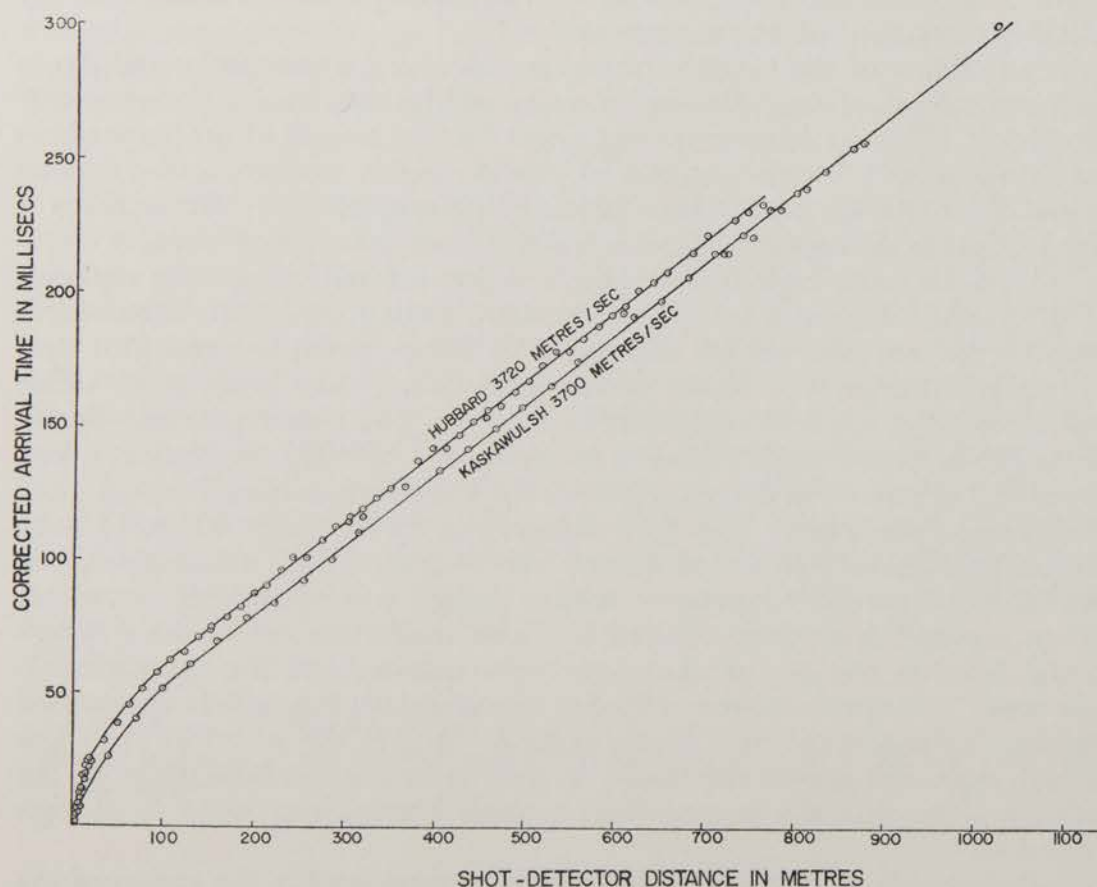


Fig. 5. Refraction arrival times.

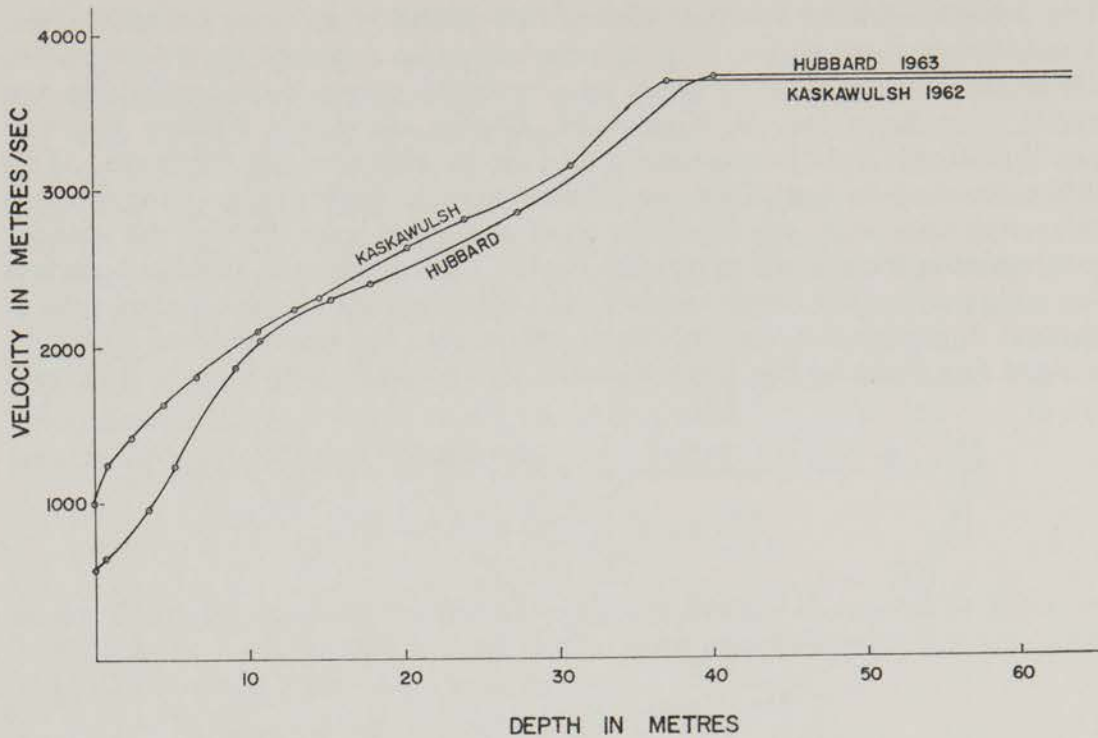


Fig. 6. Velocity of P waves with depth.

The velocity-depth relationship (Fig. 6) was computed by numerical integration of the time-distance curve obtained from refracted first arrivals (Fig. 5). From the Herglotz-Wiechert solution (Slichter, 1932) the penetration depth, Z_p , for a refracted ray arriving at a detector a distance Δ_p from the shot point is

$$Z_p = \frac{1}{\pi} \int_0^{\Delta_p} \cosh^{-1} \frac{V_p}{V_\Delta} d\Delta$$

where V_Δ is the maximum velocity corresponding to a shot-to-detector distance Δ (see Fig. 7). Because V_p is the velocity at depth Z_p the time for a wave to travel to a depth h is

$$T = \int_0^h \frac{dZ_p}{V_p}$$

When h is the thickness of the firm layer this integration permits the determination of the time required for a vertically-travelling wave to pass through this layer. The results of the two refraction surveys are summarized in Table 2 below.

Table 2. Results of seismic refraction measurements.

Glacier	Δ_p	Z_p	one-way time to Z_p	V_{surface}	V_{ice}
Kaskawulsh	130 m	37 m	0.016 sec	1010 m/sec	3700 m/sec
Hubbard	99 m	40 m	0.020 sec	576 m/sec	3720 m/sec

The determination of P-wave velocities are probably accurate to ± 20 m/sec. The velocity-depth curves (Fig. 6) deserve special comment since both curves differ in character from typical velocity-depth curves for glaciers. In the upper 10-m layer for the Kaskawulsh Glacier curve the velocity increases rapidly but this rapid increase is not seen on the Hubbard Glacier curve. This difference may be caused by the different seismic apparatus used for the two refraction lines or by the deterioration of the upper layer through the summer melting since the refraction profiles for the Kaskawulsh and Hubbard glaciers were obtained at the beginning and end of the summer ablation period respectively. Although the velocity-depth curves give the impression of a clearly-defined firn thickness this is not the case. The velocity-depth curve is derived

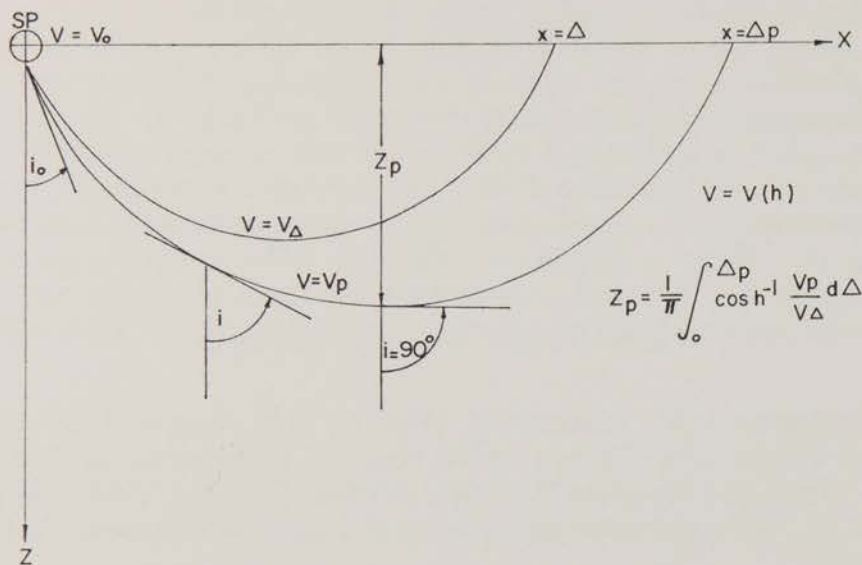


Fig. 7. Curved ray paths in the firn layer.

from the time-distance curve and the firn thickness corresponds to whatever value of Δ_p is chosen from the time-distance plot. This distance is not apparent as a sharp break on the time-distance curve. The choosing of a value of Δ_p is critical for the determination of Z_p but has a very slight effect on the calculated depths for reflection stations. Table 3 shows P-wave velocities measured on various glaciers of the world.

Table 3. Velocities of P waves in glacier ice.

Location	Reference	V_p
Taku Glacier, Alaska	Poulter, Allen, Miller ¹	3960 m/sec
Greenland Ice Cap	Bentley <i>et al.</i> (1957)	3865
Penny Icecap, Baffin Island	Röthlisberger (1955)	3810
"McGill Ice Cap", ² Axel Heiberg Island	Redpath (1961)	3790
Hubbard Glacier, Yukon Territory	Clarke	3720
Kaskawulsh Glacier, Yukon Territory	Becker (Pers. comm.)	3700
Athabasca Glacier, Alberta	Paterson and Savage (1963)	3610
		3600

¹Extracted from a table by Holtzschcher (1954).

²Now officially Akaioa Icecap.

Application of refraction results to reflection seismic results

Having found the firn thickness, the time required for a vertically-traveling wave to pass through this, and the velocity of P waves in ice, the way the firn layer is to be treated in computing the reflection results must be decided. Solving the two-layer problem for refracted wave paths is hardly warranted since these paths are nearly vertical. More practical approaches are either to strip off the firn layer by subtracting the total travel-time for vertically-traveling P waves in firn, from the times of the reflected arrivals and then calculating the thickness of glacier ice and adding to that the firn thickness, or to compute an average velocity and solve the problem as a single layer problem. Neither approach considers the effect of curved ray paths in the firn layer but the latter method is less sensitive to the effect of a thick firn layer and was therefore used for all reflection calculations. The average velocity is

$$\bar{V} = V_{ice} \left(1 - 2 \frac{T_{firn}}{T_{total}} \right) + 2 \frac{Z_{firn}}{T_{total}}$$

where T_{firn} is the one-way vertical travel time in firn and Z_{firn} the firn thickness. In the case of the n^{th} multiple reflection a wave passes through the firn layer $2(n+1)$ times and the average velocity is

$$\bar{V} = V_{ice} \left(1 - 2(n+1) \frac{T_{firn}}{T_{total}} \right) + 2(n+1) \frac{Z_{firn}}{T_{total}}$$

Since the values of the velocity for P waves in ice (Table 2) from the two refraction surveys agree within the limits of error, it was decided to use the mean value of $V_{ice} = 3710 \pm 20$ m/sec for all calculations. The values of T_{firn} and Z_{firn} for the Hubbard Glacier were used in computing \bar{V} for stakes 25 to 46 on the Hubbard Glacier. All other values of \bar{V} were found using the results from the Kaskawulsh refraction profile.

Determination of the depth and spatial orientation of a dipping plane from primary and multiple reflections

It has been established that multiple reflections are routine phenomena in glacier seismic work. It was therefore decided to interpret every supposedly reflected event both as a primary reflection, as a first multiple, and as a second multiple reflection. For simplicity of analysis the glacier was considered to be a one-layer problem in which the firn layer was accounted for by taking an average velocity. This average velocity is exact for waves travelling vertically, and becomes an increasingly poor approximation for waves of high incident angle. Energy and geometric considerations limit the likelihood of high-angle multiple reflections so that the average velocity approach is not unrealistic.

In order to determine the three coordinates which are necessary to locate a point in space (the image shot point) it is necessary to make three independent measurements. For reflection seismology the data from three geophones not in a line are therefore recorded. This requires either shooting along two separate lines or shooting once and recording from a suitable array such as an L-spread.

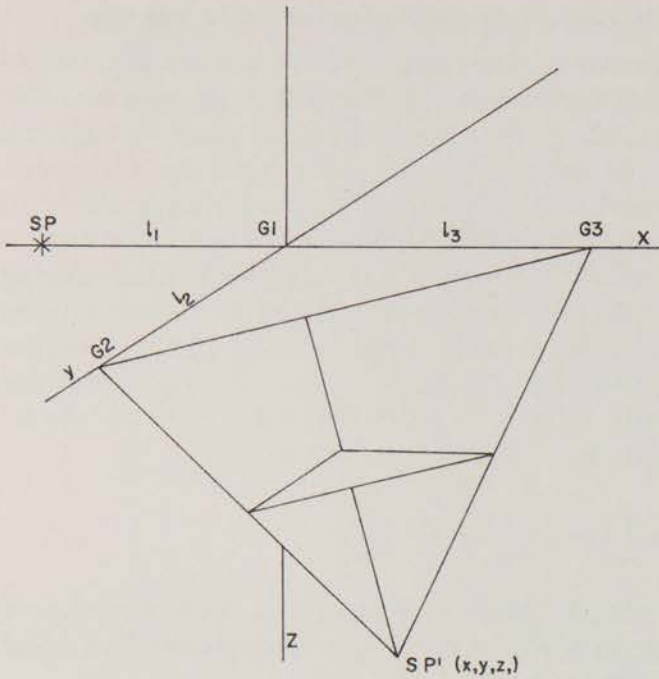


Fig. 8.
Coordinates of detectors, shot point, and image shot point.

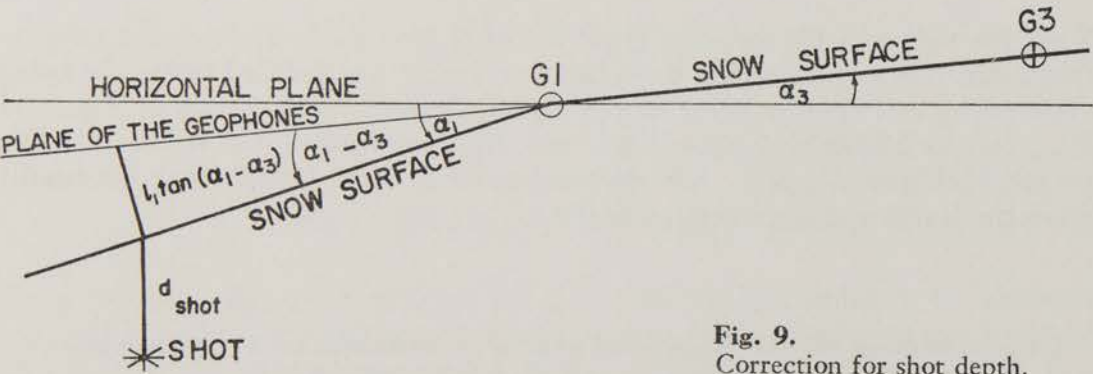


Fig. 9.
Correction for shot depth.

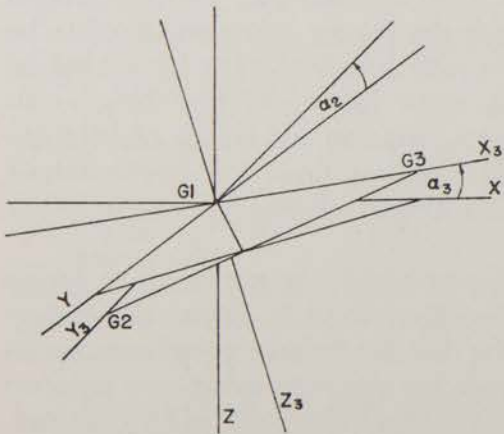


Fig. 10.
Spatial orientation of the plane of the three detectors.

A computer program was prepared to reduce all seismic reflection measurements and to find the depth and space orientation of the reflecting plane (assuming it was a plane). The program consisted of three parts:

- (1) reduction of levelling and chaining results;
- (2) application of time corrections;
- (3) computation of depth and orientation resulting from interpretation of event as a primary or a first or second multiple reflection.

The elevations of the three principal geophones and the top of the shot hole were found by levelling with a transit and stadia rod; the slope distances were determined by chaining and a knowledge of the inter-geophone spacing. The reduction of these measurements consisted merely of converting chain and level data to angles from the horizontal with respect to the apex geophone (G1 in Fig. 8), and of converting all lengths to the metric system.

Corrections to arrival times were necessary to allow for the time lapse between the first break of a reflected arrival and the first trough of the wavelet. The first trough was the arrival picked from the records in all cases, since it is the most easily distinguished. The time interval between the first break and the first trough was measured from a number of high quality records, averaged and applied as a correction to all records. The extensive filtering required for "clean" records proved a dubious asset since transmission time curves subsequently supplied by the manufacturer indicated that the transmission times were of the order of 20 msec for the filter settings used, and that the delay time was quite sensitive to the frequency of the wave. This injects an unknown into all records and presents a strong case for restricted use of filters. From the five routinely used filter settings average reflected frequencies were computed from all records for each group. This average frequency was taken as the frequency which characterized the particular filter setting and from this frequency a single lag time was computed for each filter setting and applied as a correction to all records with the same filter settings (Table 4).

Table 4. Filter data.

<i>Filter setting</i>	<i>No. of frequency picks</i>	<i>Spread in frequency</i>	<i>Mean frequency</i>	<i>Delay time</i>
MM90 - M140	2	105-142 cps	124 cps	0.020 sec
MM70 - M140	27	88-114	103	0.017
MM40 - M140	1	86	86	0.015
MM40 - M90	68	58-118	76	0.025
MM50 - M90	14	61- 91	78	0.023

Finally a correction for shot depth was applied. This consisted of two parts: a correction to place the shot at the surface and a correction to place the shot from the surface to the plane of the three detectors. From the two refraction profiles an average velocity for P waves at the surface was found to be 793 m/sec and the distance which the shot had to be moved was divided by this velocity to give a time correction. From Fig. 9 this correction is seen to be approximately

$$t_{\text{shot}} = \frac{d_{\text{shot}}}{V_{\text{surface}}} + \frac{l_1 \tan(\alpha_1 - \alpha_3)}{V_{\text{surface}}}$$

and this was added to the reflection arrival times.

Assume that the shot point and the three detectors are coplanar and have coordinates

$$\begin{aligned} G1 &: (0,0,0) \\ G2 &: (0,l_2,0) \\ G3 &: (l_3,0,0) \\ SP &: (-l_1,0,0) \end{aligned}$$

with the apex of the L-spread at the origin (Fig. 8) and let the unknown coordinates of the image shot point be x, y, z . Considering the velocity as constant and denoting the time required for a wave to travel from the image shot point to detectors $G1, G2$, and $G3$ as t_1, t_2, t_3 respectively, the resulting expressions are

$$V^2 t_1^2 = x^2 + y^2 + z^2 \quad (1)$$

$$V^2 t_2^2 = x^2 + (y - l_2)^2 + z^2 \quad (2)$$

and

$$V^2 t_3^2 = (x - l_3)^2 + y^2 + z^2 \quad (3)$$

Solving (1) and (2) for y yields

$$y = \frac{V^2 (t_1^2 - t_2^2) + l_2^2}{2l_2}$$

and (2) and (3) for x ,

$$x = \frac{V^2 (t_2^2 - t_3^2) + 2yl_2 + l_3^2 - l_2^2}{2l_3}$$

and finally from (1),

$$z = \sqrt{V^2 t_1^2 - x^2 - y^2}.$$

If the three detectors are not in the horizontal plane then the results must be transformed to place the three detectors in their correct orientation (Fig. 10). (The previously discussed shot-depth correction renders the shot point coplanar with the three geophones.) Assuming the angles from the horizontal to be small, the transformation can be approximated by successive transformations. First rotate the axes about the y axis by an angle α_3 , the angle which the line joining $G1$ and $G3$ makes with the horizontal plane. Then rotate the resulting axes about the new x axis by the angle α_2 , the angle the original y axis made with the horizontal. The resulting transformations are

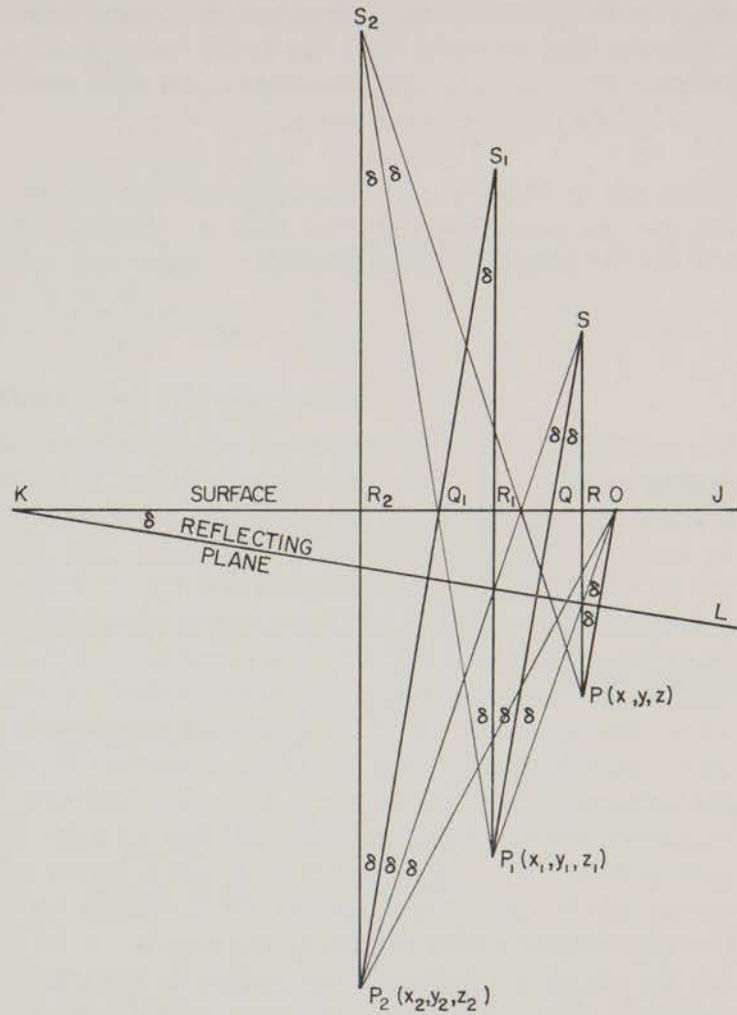
$$\begin{aligned} x_1 &= x \cos \alpha_3 + z \sin \alpha_3 \\ y_1 &= y \\ z_1 &= x \sin \alpha_3 + z \cos \alpha_3 \\ x_2 &= x_1 = x \cos \alpha_3 + z \sin \alpha_3 \\ y_2 &= y \cos \alpha_2 + z_1 \sin \alpha_2 = x \sin \alpha_3 \sin \alpha_2 + y \cos \alpha_2 + z \cos \alpha_3 \sin \alpha_2 \\ z_2 &= y_1 \sin \alpha_2 + z_1 \cos \alpha_2 = x \sin \alpha_3 \cos \alpha_2 + y \sin \alpha_2 + z \cos \alpha_3 \cos \alpha_2. \end{aligned}$$

Finally translate the shot point to the origin

$$\begin{aligned} x_3 &= x \cos \alpha_3 + l_1 + z \sin \alpha_3 \\ y_3 &= y_2 \quad z_3 = z_2. \end{aligned}$$

Having now obtained the coordinates of the image shot point the depth, dip, and dip direction may be determined. The depth is merely half the value of the z_3 coordinate. The strike of the dip with respect to the axes (Fig. 8)

Fig. 11.
Multiple reflections from
a dipping plane.



is in the direction of the horizontal projection of the line joining the shot point to the image shot point and is therefore

$$\theta = \tan^{-1} \left(\frac{y_3}{x_3} \right).$$

The dip angle is

$$\delta = \tan^{-1} \left(\frac{\sqrt{(y_3)^2 + (x_3)^2}}{z_3} \right).$$

The foregoing calculations may be readily extended to computation for multiple reflections. The problem reduces to that of finding the trigonometric relationship between the image shot points for the primary and multiple reflections.

Consider a plane in space dipping at an angle δ with respect to the horizontal plane (Fig. 11). The shot point is located at point O on the surface. Waves are reflected at the two boundary planes so that the waves reflected from the dipping plane will arrive as if propagated from an image source located at point P . The method of images locates the image shot points for the first and second multiple reflections these image sources being $P_1(x_1, y_1, z_1)$ and $P_2(x_2, y_2, z_2)$ respectively. The subscripts in this notation are not to be confused with the

usage in the previous section to indicate transformation of coordinates. The angles labelled as equal to δ are easily recognized using the fact that for an isosceles triangle the angles opposite equal sides are equal.

For the first reflected arrival

$$\tan^{-1} \frac{\overline{OR}}{\overline{RP}} = \frac{\sqrt{x^2 + y^2}}{z} = \delta$$

and for the first multiple reflection

$$\tan^{-1} \frac{\overline{OR_1}}{\overline{R_1P_1}} = \tan^{-1} \frac{\sqrt{x_1^2 + y_1^2}}{z_1} = 2\delta$$

$$\tan^{-1} \frac{\overline{QR_1}}{\overline{R_1P_1}} = \delta$$

so that

$$\overline{R_1Q} = \overline{R_1P_1} \tan \delta = z_1 \tan \delta$$

$$\overline{QO} = 2\overline{RP} \tan \delta = 2z \tan \delta$$

$$\overline{OR_1} = \sqrt{x_1^2 + y_1^2} = \overline{R_1Q} + \overline{QO} = z_1 \tan \delta + 2z \tan \delta.$$

Solving for z ,

$$z = \frac{\frac{1}{2}(\tan 2\delta - \tan \delta) z_1}{\tan \delta}$$

and

$$z_1 = \frac{2z \tan \delta}{\tan 2\delta - \tan \delta}$$

The dip direction with respect to the axes is

$$\theta_1 = \tan^{-1} \frac{y_1}{x_1}$$

and the depth can be found as before using the relationship between z_1 and z . Similarly for the second multiple reflection with image shot point

$$P_2(x_2, y_2, z_2),$$

$$\tan^{-1} \frac{\overline{OR_2}}{\overline{P_2R_2}} = 3\delta = \tan^{-1} \frac{\sqrt{x_2^2 + y_2^2}}{z_2}$$

$$\overline{Q_1R_2} = \overline{P_2R_2} \tan \delta = z_2 \tan \delta$$

$$\overline{QQ_1} = \overline{Q_1R_1} + \overline{R_1Q} = 2\overline{R_1Q} = 2P_1R_1 \tan \delta$$

and

$$\overline{QO} = \overline{QR} + \overline{RO} = 2\overline{RO} = 2z \tan \delta$$

$$\overline{OR_2} = \overline{Q_1R_2} + \overline{Q_1Q} + \overline{QO} = \sqrt{x_2^2 + y_2^2} = z_2 \tan \delta + 2z_1 \tan \delta + 2z \tan \delta.$$

Using the previously derived relation for z_1 ,

$$\sqrt{x_2^2 + y_2^2} = z_2 \tan \delta + \frac{4z \tan^2 \delta}{\tan 2\delta - \tan \delta} + 2z \tan \delta$$

$$z = \frac{z_2 (\tan 3\delta - \tan \delta) (\tan 2\delta - \tan \delta)}{2 \tan \delta (\tan 2\delta + \tan \delta)}$$

The depth follows immediately from the previously derived relations, and the strike is

$$\theta_3 = \tan^{-1} \frac{y_3}{x_3}$$

with respect to the axes. For the one layer case $\theta_1 = \theta_2 = \theta_3$ but in the above treatment a different average velocity is used for each reflection so that the values of θ change slightly for the primary and multiple reflections.

Results of seismic survey

The results of the computer program to determine the ice thickness are summarized in Clarke (1964); the bedrock profiles for the entire area of coverage are shown in Fig. 12; the bedrock contours for a smaller area of detailed coverage are included in Fig. 13. Since the reflection times for a record of good quality may be estimated to ± 1 msec the resulting uncertainty in ice thickness is ± 2.0 m. Considering the uncertainties in the filter correction and variations in the time between the first break and the first trough of a reflected arrival, the accuracy for relative differences in ice thickness should be within ± 10 m. Occasionally the arrival time may be in error by one complete cycle, which would cause an error of the order of 25 m in the ice thickness. The estimated accuracy of the absolute values of ice thickness are dependent on the accuracy of the average velocity and the faith one places in the manufacturer's transit time estimates which seem inordinately high. It would appear that the absolute values of ice thickness are within 5 per cent of the actual values.

The resulting ice thicknesses for all reflections identified are shown on the profiles; reflections of low quality which indicate a bedrock profile differing from that indicated by gravity are identified as poor quality reflections. In all cases the reflecting points are projected on to the plane of the profile, for instance the profile may indicate a bedrock high, but the actual cause is frequently that the line of the profile does not exactly follow the valley centre and reflections from the valley sides are being received. When the reflecting surface was found to be more than 100 m from the line of the profile such reflections were indicated as oblique. On a number of records more than one reflected event was identified. These included supposed multiple reflections from several image sources as well as possible moraine reflections. Not infrequently the various reflections provided valuable additional information from distant reflecting surfaces so that one shot might provide ice thickness information from as many as three distant locations. This was particularly evident from the cross traverses for which the first reflected arrival was an oblique shadow reflection from the valley side followed by deeper less oblique reflections from nearer the valley centre. In every case the bedrock surface was determined from the shallowest reflection received except when the first reflection was oblique and a near vertical reflection followed. At several stations gravity profiles differed greatly from the seismic profile and also the seismic depth was not consistent with the trends and adjacent values—the depth being greater than expected. In such cases the depth values assuming a first

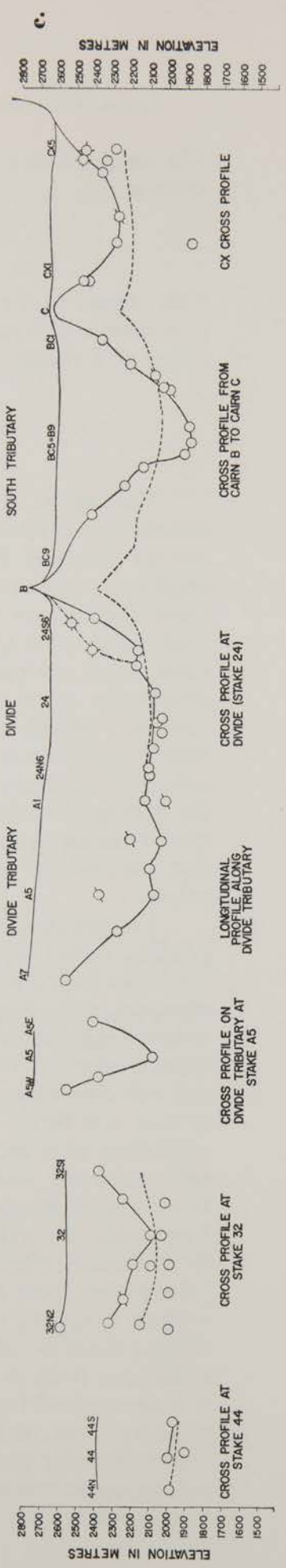
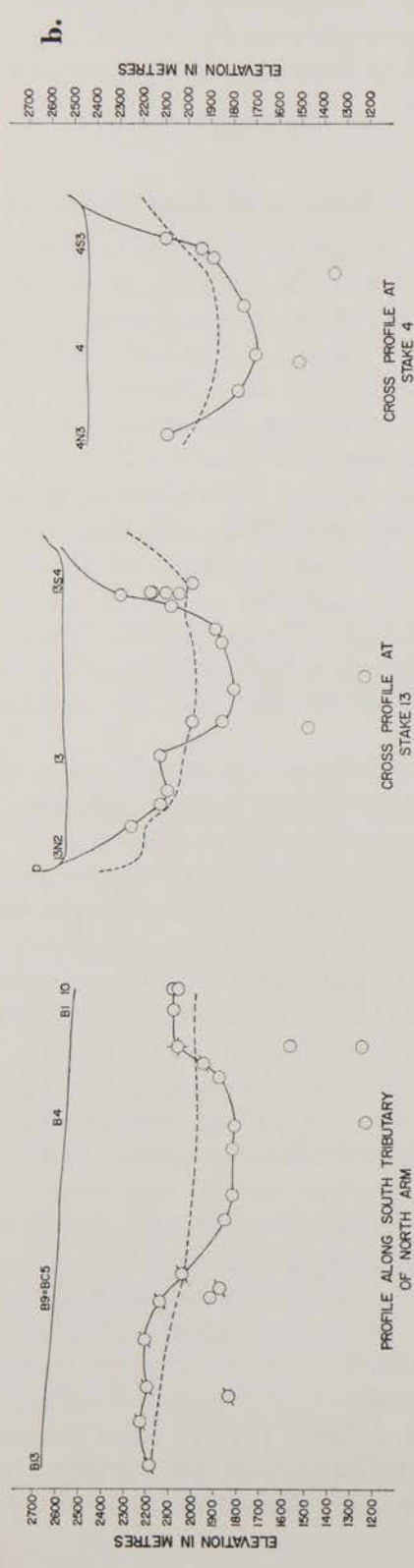
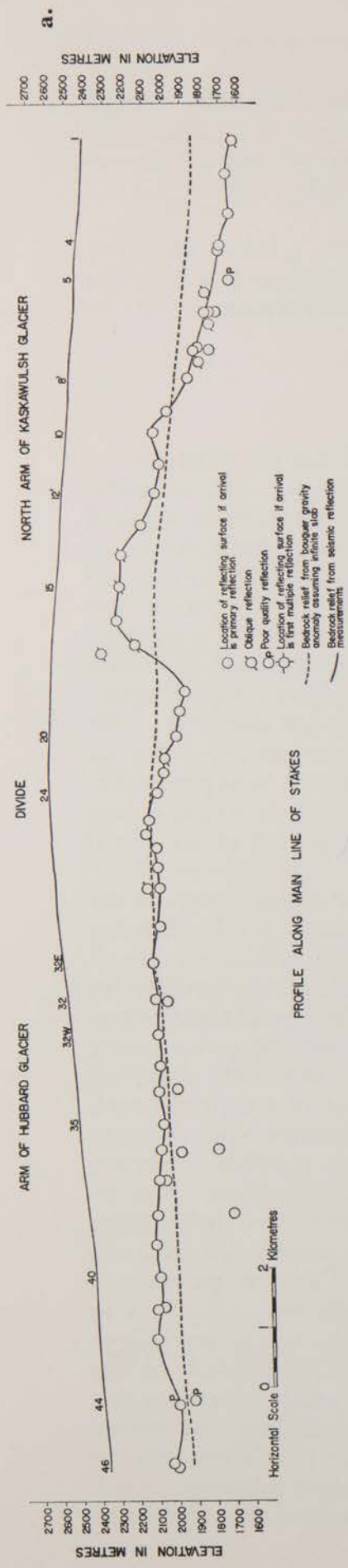


Fig. 12 a, b, c.
Bedrock profiles from geophysical measurements.

or second multiple reflection was calculated. If the resulting value fitted the gravity profile and bedrock trends it was accepted and was indicated as a depth obtained from a multiple reflection. The depths for stations at B2 and CX5 are examples of calculations made assuming the reflected event to be a first multiple reflection. The bedrock surface resulting if the reflections at stations 24S5 and 24S6' are first multiples is dotted in but the evidence for this is dubious.

Records with several reflected events which seem likely to be multiples can be used to test the method of ice thickness calculation. At stake CX2 events at 242 msec and 462 msec were detected. Assuming the first event to be a primary reflection the ice thickness is 362 m. Assuming the second event to be a first multiple reflection gives an ice thickness of 376 m. At stake B2 events at 576 msec and 746 msec give thicknesses of 481 m and 419 m, assuming these to be first and second multiple reflections, the primary reflection being obscured. The poor coincidence of the last values may be due to several causes. For instance, the primary assumptions may be invalid, or the reflecting surface is not a plane, or the reflections may not be simple multiples as assumed.

INVESTIGATIONS OF GLACIER FLOW

Measurements of surface flow on the Kaskawulsh and Hubbard glaciers

Annual and summer surface flow rates have been determined from three surveys of the metal stakes erected in 1962. The first survey was made by Zissett in 1962; two surveys were made by Sharni in 1963 (Survey I and Survey II). A Wild T2-400" theodolite was used and coordinates were found by resection and intersection. The coordinates of the 1963 survey are estimated to be correct to within ± 30 cm and the elevations to be within ± 10 cm at the time of the survey. The annual flow rates for the metal stakes are found in Table 5 and a part of Sharni's map of flow vectors is reproduced (Fig. 13). Values in Table 5 which are believed erroneous or of low accuracy are indicated by brackets. The summer flow rate proved to be the same as the mean annual flow rate on the Kaskawulsh Glacier but greater than the mean annual flow rate on the Hubbard Glacier. This latter observation may be due entirely or in part to differences in the date of survey, the stakes on the Hubbard Glacier having been erected near the end of the summer of 1962, whereas those on the Kaskawulsh were erected early in the summer. The maximum annual movements were 150 m at stake 1 on the Kaskawulsh Glacier and 132 m at stake 44 on the Hubbard Glacier.

The relationship of surface flow to ice thickness measurements

The close relationship that exists between bedrock topography and surface flow is shown in Fig. 13 in which the geophysically-determined ice thicknesses form the control points on a contour map of the bedrock surface on to which is superimposed a map of the surface flow vectors. The bedrock surface was contoured from the geophysically-determined ice thicknesses. The flow line and the line of the valley centre are roughly coincident. On the Hubbard Glacier the flow line closely follows the line of marker stakes whereas on the Kaskawulsh Glacier the line of stakes is offset from the flow line. Tributary glaciers deflect the flow of the main channel and at the divide the flow is complicated by the swirl effect of the Divide Tributary.

When seismic investigations were first planned in the divide area of the Kaskawulsh and Hubbard glaciers the question of whether or not a bedrock divide could be related to the flow divide was considered. After two summers of seismic measurements the answer is still not clear. It is often difficult to know whether seismic measurements have been made at the deepest point of the valley cross-section. Perhaps the best plan would be to measure ice thickness along the flow line which should coincide with the deepest channel. In Nye's (1952 a, b) discussion of the relative influences of surface slope and bedrock slope in determining surface flow it is made clear that the surface slope is the more significant factor. Hence the observed coincidence of the flow divide with the topographic divide is to be expected but there is no reason to

Table 5. Annual movements of flow stakes.

$$\Delta x = x_{63} - x_{62}$$

$$\Delta y = y_{63} - y_{62}$$

$$\Delta v^2 = \Delta x^2 + \Delta y^2$$

Stake	Δx ($x_{63} - x_{62}$)	Δy ($y_{63} - y_{62}$)	Δv ($\sqrt{\Delta x^2 + \Delta y^2}$)
1	143.1 <i>m</i>	45.6 <i>m</i>	150
2	127.5	40.0	134
3	111.3	50.7	123
4	103.4	54.0	117
5	95.7	58.7	112
6	87.3	58.2	105
7	76.5	51.0	92
8'	—	—	(85)
9	67.3	35.9	76
10	60.4	32.7	69
11	54.1	28.3	61
12'	—	—	(53)
13	40.6	18.3	45
13S	48.3	32.1	58
13N	34.8	8.7	36
14	35.1	14.3	38
15	33.7	6.5	34
16	29.2	-0.4	29
17	(66.8)	(35.1)	(22)
18	21.7	-6.4	23
19	20.2	-6.6	21
20	16.8	-7.0	18
21	15.8	-12.2	20
22	12.4	-8.8	15
23	9.6	-8.8	13
24	0.7	-8.1	8
24S5	4.3	-2.3	5
24S4	2.5	-1.4	3
24N4	0.9	-22.4	22
24N5	8.5	-31.8	33
24N6	20.7	-34.3	40
25	-14.4	-8.2	17
26	-16.2	-7.8	18
27	-18.5	-7.6	20
28	-22.5	-7.2	24
29	-26.8	-6.1	27
30	-30.4	-7.8	31
31	-34.4	-7.7	35
32E	-37.8	-14.3	40
32	-44.1	-23.0	50
32W	-59.1	-22.9	63
32S	-33.4	-10.1	35
32N	-41.8	-29.8	51
33	-71.4	-24.9	76
34	-74.7	-28.5	80
35	-79.5	-35.6	87
36	-84.0	-47.7	97
F14	-85.7	-50.7	100
37	-80.4	-54.5	97
38	—	—	(126)
39	-86.9	-69.8	111
40	-98.8	-65.5	118
41	—	—	(155)
42	-114.9	-60.5	130
43	-117.0	-58.8	131
44	-120.6	-54.6	132
45	-118.3	-51.1	129
46	-115.4	-46.7	125

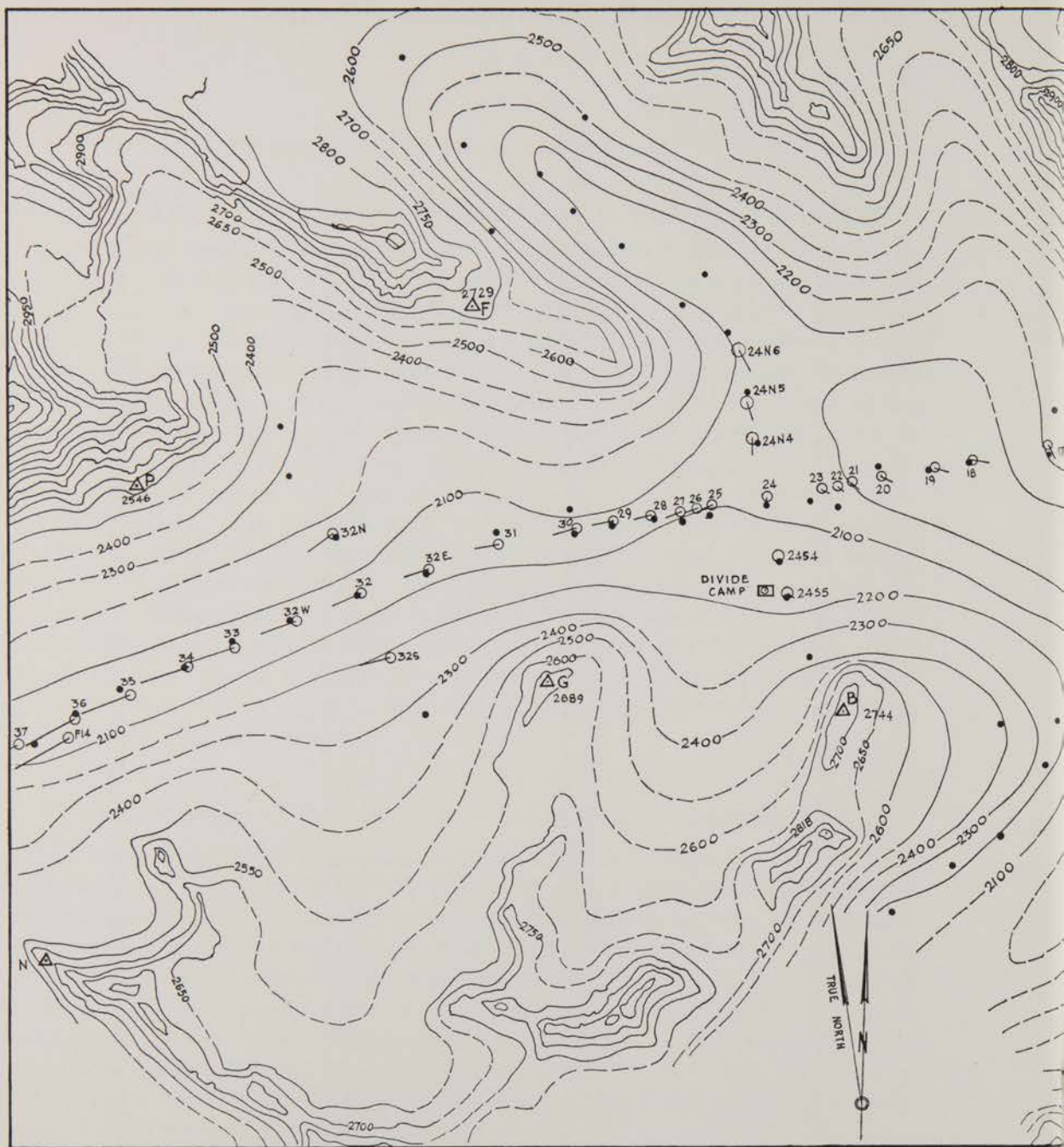
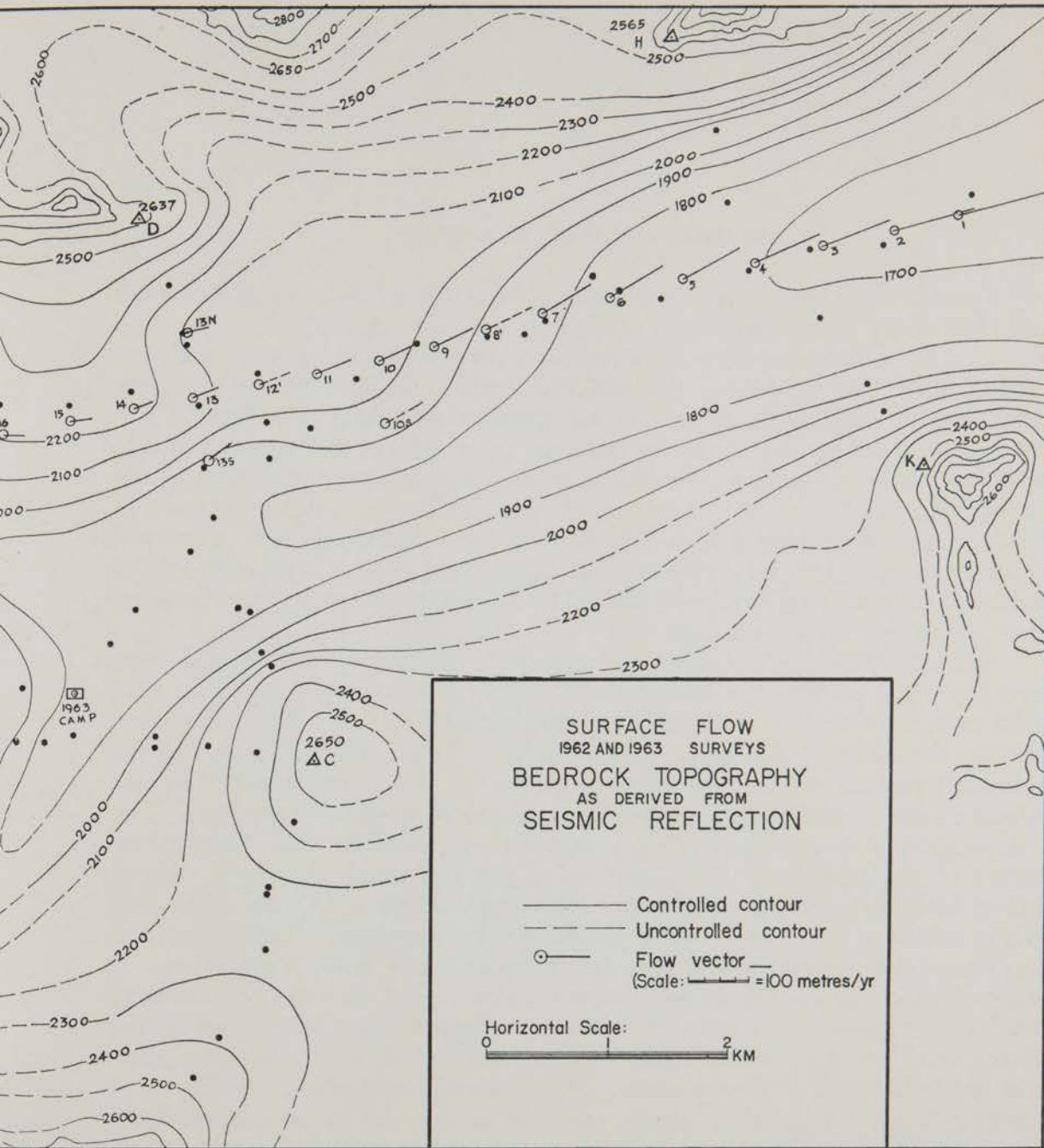


Fig. 13. Bedrock topography

expect a corresponding bedrock divide. Indeed, dismissing the bedrock high between stake 17 and stake 8 as being well displaced from the valley centre, the glacier trough would appear to be highest at stake 39 on the Hubbard Glacier. This is hardly a clearly-defined divide, and it seems better to think of a divide in a broader sense and not as a sharply-defined high in the bedrock.

An interesting relationship between surface elevation and bedrock topography is found in the vicinity of stake 41 near the end of the line of stakes on the Hubbard Glacier. A high in the surface elevation between stakes 40 and 42 appears to result from a bedrock high at stake 42 "downstream" from the



d surface flow rates.

surface wave. In addition the downslope rate of increase of surface flow suddenly decreases from a fairly uniform rate of the order of 12 m/yr per km downslope to a value near zero. In other words the flow changes from extending to non-extending. Unfortunately discrepancies in both the seismic results and the flow measurements preclude any detailed analysis of these relationships and this would seem to be an area in which further study could prove very rewarding. Detailed seismic work in the vicinity of the flow divide between the arms of the Kaskawulsh and Hubbard glaciers in conjunction with flow measurements on the Divide Tributary would also be of value.

SUMMARY AND CONCLUSIONS

From gravity and seismic measurements near the divide of the Kaskawulsh and Hubbard glaciers calculations of ice thickness were made.

Gravity differences were measured for a network of 107 stations and corrections made for misclosure, latitude, and terrain. In spite of the great uncertainties in making three-dimensional terrain corrections in a largely ice-covered area, the gravity anomalies observed were sufficiently pronounced that errors in terrain correction were not critical except for gravity stations at the cairns. An absolute gravity base was obtained indirectly using a tie made in 1962 to a geodetic station at Kluane Village on the Alaska Highway. Observed Bouguer anomalies in the divide region ranged from -199.8 mgal over ice (at stake B6) to -162.9 mgal on rock (cairn D) indicating a large negative Bouguer anomaly for the St. Elias Range.

Seismic reflections were obtained at most of the gravity stations and from two refraction profiles the velocity of P waves in ice was found to be 3710 ± 20 m/sec. The firn thickness was approximately 40 m and the minimum velocity found in the firn layer was 576 m/sec. From an investigation of the maximum possible effects of anisotropy in the ice it was concluded that any effects on the refraction results would be sufficiently small to be ignored. The computation of an average vertical velocity at each seismic station from calculations of the time delay and thickness of the firn layer was made. Using arrival times from three geophones not in a line the depth and spatial orientation of the reflecting surface was found assuming it to be a plane. This calculation was repeated assuming the arrival to be a first or second multiple reflection. A comparison of the depths obtained from a single record on which events were identified as primary and multiple reflections suggested that either some of the events were wrongly identified or that the assumption of a reflecting plane was not satisfactory. The maximum ice thickness was found to be 778 m at stake 1 on the Kaskawulsh Glacier and 539 m at stake 29 on the Hubbard Glacier. The ice thickness at stake 24 on the topographic divide was 539 m. Maximum bedrock elevations on the main line of stakes were found to be 2261 m at stake 16 and 2102 m at stake 39 on the Kaskawulsh and Hubbard glaciers respectively.

Bouguer anomaly profiles were compared with the corresponding seismic profiles and direct comparisons of the ice-thickness determinations were made assuming the glacier to be an infinite slab. This assumption proved to be a poor approximation and effectively smoothed out bedrock relief. Because regional gravity gradients and the regional density were not well-established and because of the general high quality of the seismic reflection results no further refinements were applied to the gravity results. Nevertheless Bouguer anomaly profiles proved an invaluable aid to seismic interpretation.

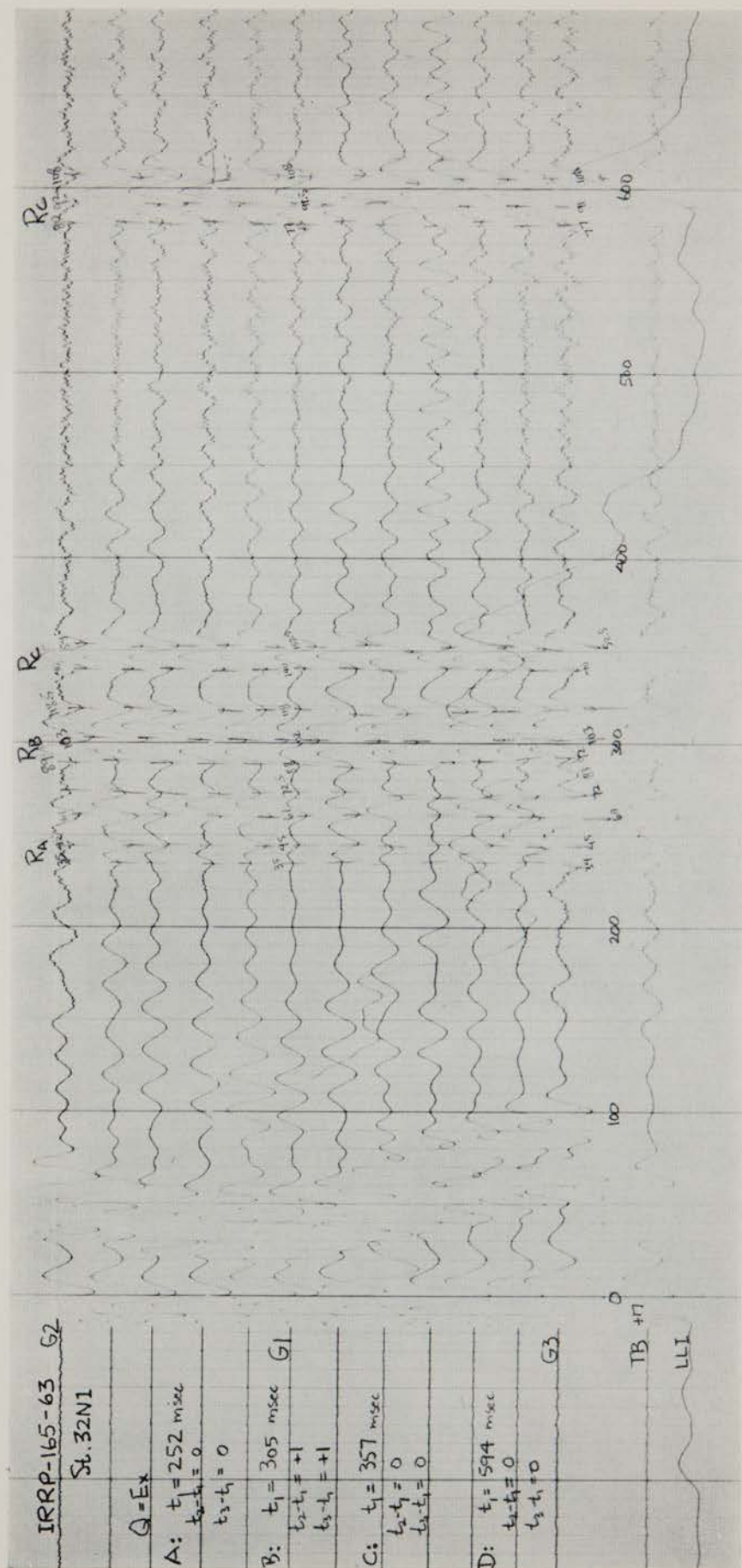


Fig. 14a. Seismic records.

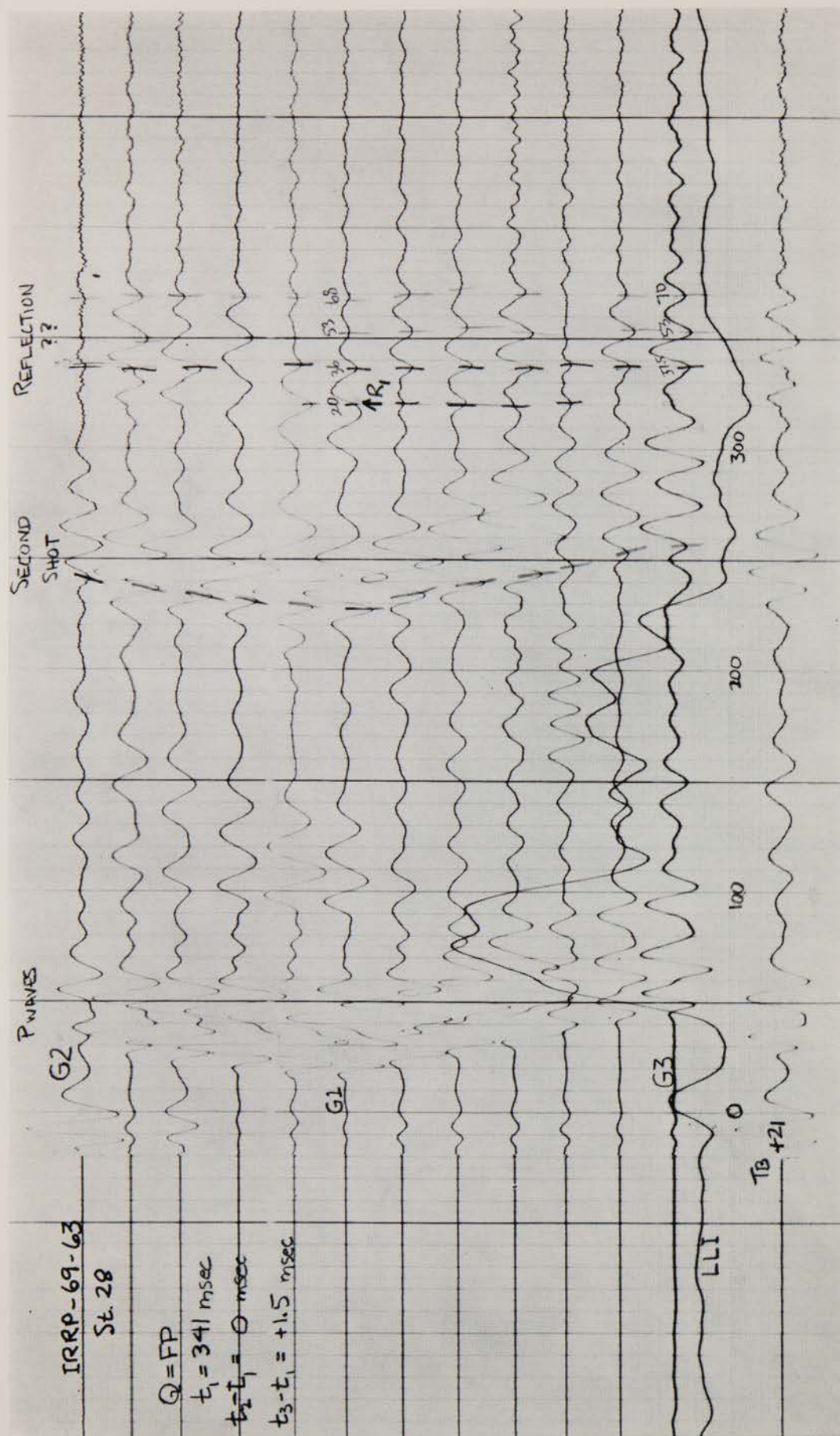


Fig. 14b. Seismic records.

From the combined gravity and seismic results the bedrock surface was contoured and the boundary of the glacier mapped. Superposition of the flow vectors established from the 1962 and 1963 surveys of the metal stakes showed a clear relationship between the surface flow and the bedrock topography. Maximum annual flow rates were found to be 150 m/yr at stake 1 on the Kaskawulsh Glacier and 132 m/yr at stake 44 on the Hubbard Glacier. The minimum measured flow was 3 m/yr at stake 24S4.

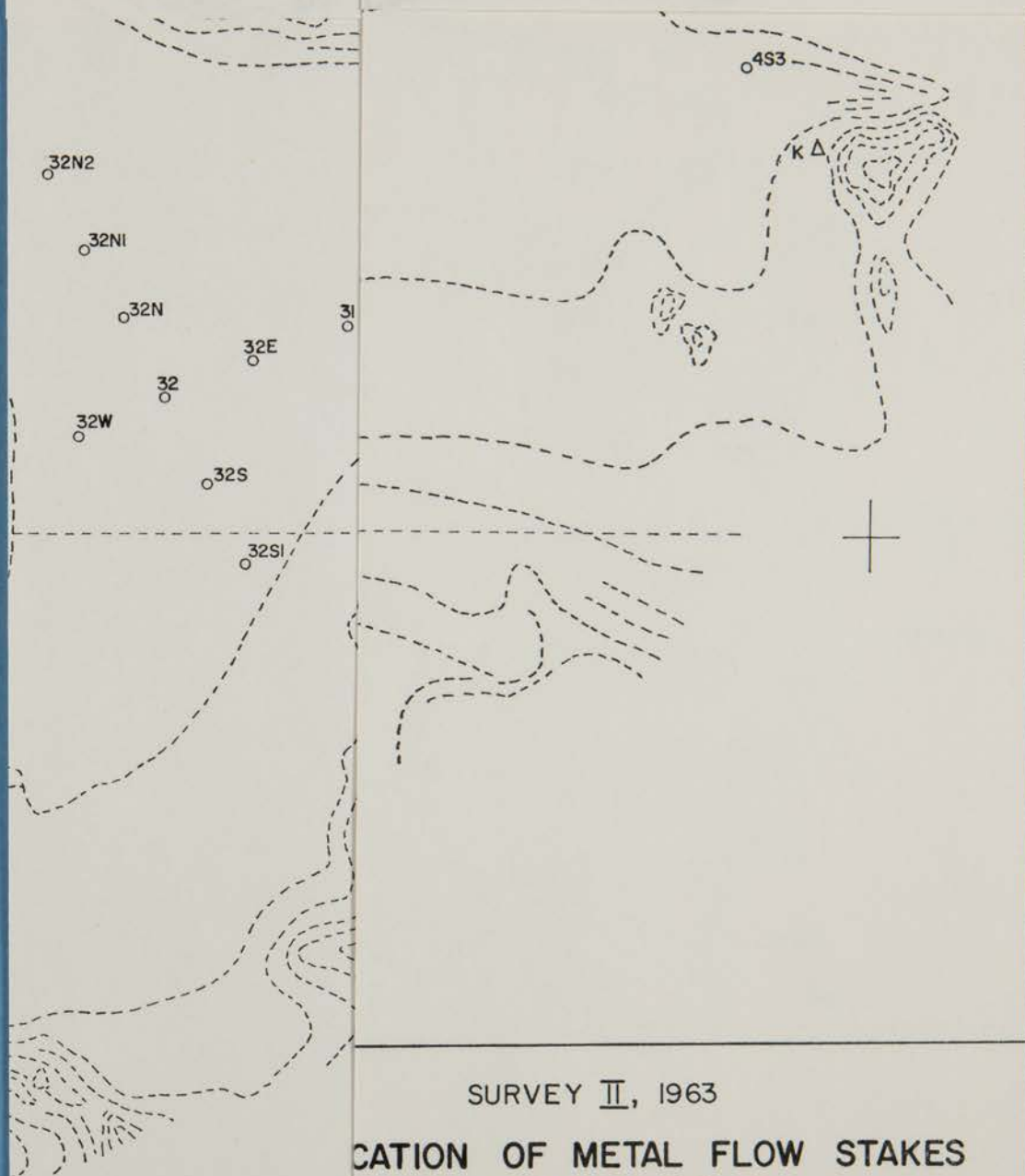
Acknowledgments

The guidance and suggestions of Prof. G. D. Garland and helpful discussions with Prof. J. C. Savage of the University of Toronto are gratefully acknowledged. To all members of the Icefield Ranges Research Project I am indebted, particularly to project leader R. H. Ragle, my stoic assistants William Isherwood and Donald Macpherson, and to Dan Sharni the project surveyor. I was supported by a National Research Council grant throughout this work. Logistic support was received from the Arctic Institute of North America, the American Geographical Society, the Defence Research Board, and the Universities of Alberta and Toronto.

References

- Ahlmann, H. W. 1933. "Part VIII. Glaciology" pp. 161-216 in 'Scientific results of the Swedish-Norwegian Arctic Expedition in the summer of 1931'. *Geografiska Annaler*, Vol. 15, 351 pp.
- Bader, H., R. Haefeli, *et al.* 1954. 'Snow and its metamorphism'. U.S. Army SIPRE, *Translation* 14, xix + 313 pp.
- Benson, C. S. 1962. 'Stratigraphic studies in the snow and firn of the Greenland Ice Sheet'. U.S. Army SIPRE, *Res. Rept.* 70, x + 93 pp.
- Bentley, C. R., P. W. Pomeroy, and J. H. Dorman. 1957. "Seismic measurements on the Greenland Ice Cap". *Ann. de Géophys.* Vol. 13, No. 4, pp. 253-85.
- Bostock, H. S. 1948. 'Physiography of the Canadian Cordillera, with special reference to the area north of the fifty-fifth parallel'. *Geol. Surv. Can. Mem.* 247, 106 pp.
- Clarke, G. K. C. 1964. 'Geophysical measurements on the Kaskawulsh and Hubbard glaciers, Yukon Territory, Canada'. M.A. Thesis, University of Toronto, 102 pp.
- Garland, G. D. 1956. "Gravity and isostasy". *Handbuch der Physik*, Vol. 47, pp. 202-45.
- Garland, G. D. and J. G. Tanner. 1957. 'Investigations of gravity and isostasy in the southern Canadian Cordillera'. *Publ. Dom. Observatory*, Vol. 19, No. 5, pp. 169-222.
- Gibson, M. O. 1941. "Network adjustment by least squares—alternative formulation and solution by iteration". *Geophysics*, Vol. 6, No. 2, pp. 168-79.
- Havens, J. and D. E. Saarela. 1964. "Exploration meteorology in the St. Elias Mountains". *Icefield Ranges Research Project 1963, Prelim. Rept.* (Unpubl.)
- Heiskanen, W. A. and F. A. Vening Meinesz. 1958. 'The earth and its gravity field'. New York: x + 470 pp.
- Holtzschcherer, J. J. 1954. "V. Seismic investigations in Inglefield Land", pp. 267-99 in 'Final report, the scientific program, Program B, Operation Ice Cap 1953'. U.S. Transportation Corps, 457 pp.
- Hubbert, M. K. 1948a. "A line-integral method of computing the gravimetric effects of two-dimensional masses". *Geophysics*, Vol. 13, No. 2, pp. 215-25.
- 1948b. "Gravitational effects of two-dimensional topographic features". *Geophysics*, Vol. 13, No. 2, pp. 226-54.

- Love, A. E. H. 1944. 'A treatise on the mathematical theory of elasticity'. New York: xviii + 643 pp.
- Nettleton, L. L. 1940. 'Geophysical prospecting for oil'. New York: xi + 444 pp.
- Nye, J. F. 1952a. "The mechanics of glacier flow". *J. Glaciol.* Vol. 2, No. 12, pp. 82-93.
- 1952b. "A comparison between the theoretical and the measured long profile of the Unteraar Glacier". *J. Glaciol.* Vol. 2, No. 12, pp. 103-7.
- Oldham, C. H. G. 1958. "Gravity and magnetic investigations along the Alaska Highway". *Publ. Dom. Observatory*, Vol. 21, No. 1, pp. 1-22.
- Paterson, W. S. B. and J. C. Savage. 1963. "Geometry and movement of the Athabasca Glacier". *J. Geophys. Res.* Vol. 68, No. 15, pp. 4513-20.
- Ragle, R. H. 1964. "The Icefield Ranges Research Project, 1963". *Arctic*, Vol. 17, No. 1, pp. 55-7.
- Redpath, B. B. 1961. "Seismic operations" pp. 101-7 in 'Jacobsen-McGill Arctic Research Expedition to Axel Heiberg Island, Queen Elizabeth Islands'. *Prelim. Rept. 1959-1960*, McGill Univ. 219 pp.
- Röthlisberger, H. 1955. "Studies in glacier physics on the Penny Ice Cap, Baffin Island, 1953. Part III: Seismic sounding". *J. Glaciol.* Vol. 2, No. 18, pp. 539-52.
- Slichter, L. B. 1932. "The theory of the interpretation of seismic travel-time curves in horizontal structures". *Physics*, Vol. 3, pp. 273-95.
- Sharni, D. 1963. "Survey report 1963". *Icefield Ranges Research Project*. (Unpubl.)
- Talwani, M. and M. Ewing. 1960. "Rapid computation of gravitational attraction of three dimensional bodies of arbitrary shape". *Geophysics*, Vol. 25, pp. 203-25.
- Wood, W. A. 1963. "The Icefield Ranges Research Project". *Geogr. Rev.* Vol. 53, No. 2, pp. 163-84.



SURVEY II, 1963

LOCATION OF METAL FLOW STAKES AND SEISMIC STAKES

Scale in Kilometres



Δ Triangulation Cairn

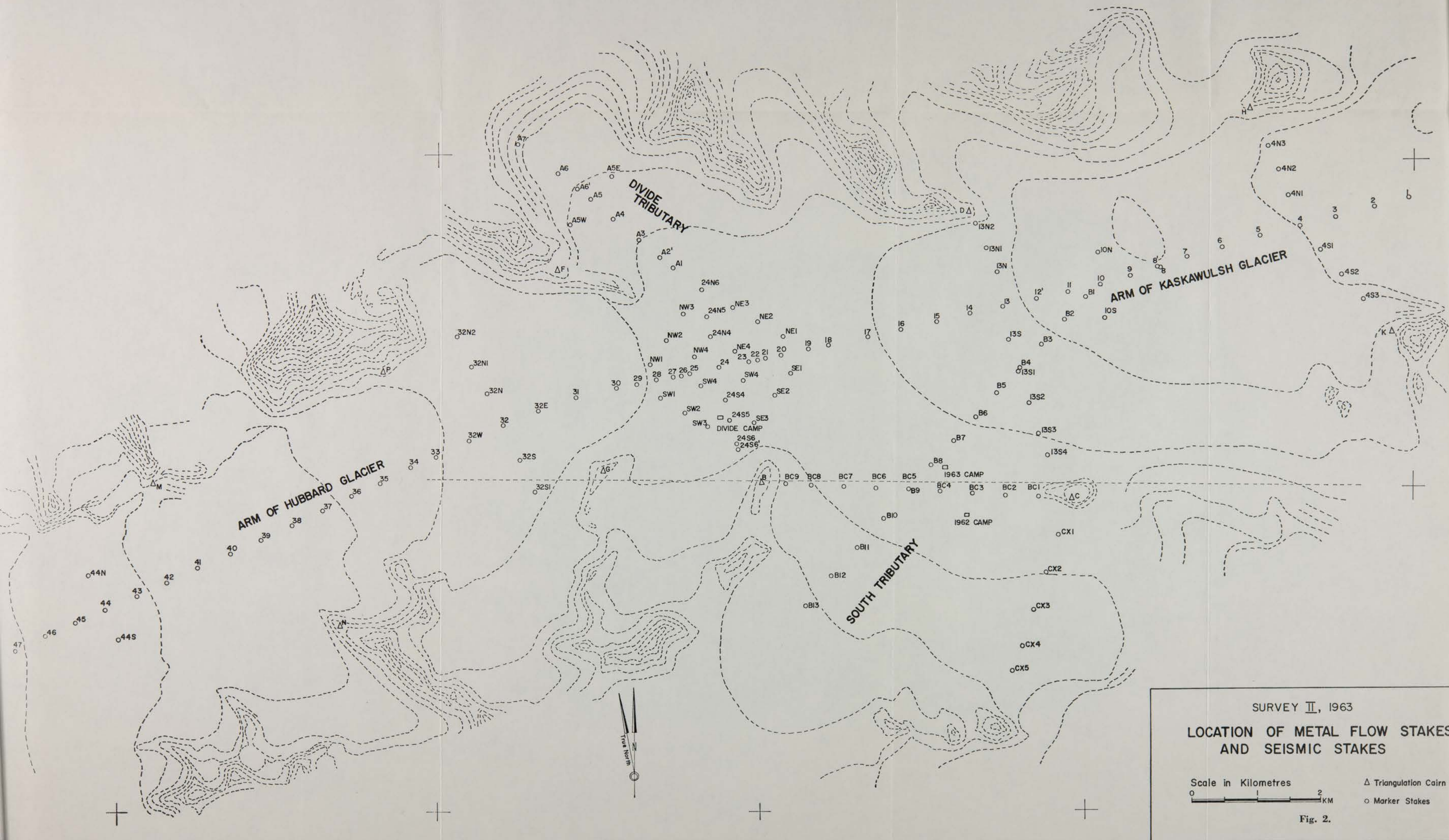
○ Marker Stakes

Fig. 2.

TECHNICAL PAPERS OF THE ARCTIC INSTITUTE OF NORTH AMERICA

Copies of the *Technical Papers* can be obtained from the Montreal Office of the Institute, 3458 Redpath Street, Montreal 25, P.Q., Canada.

- Number 1. THE PLANKTON OF THE BEAUFORT AND CHUKCHI SEA AREAS OF THE ARCTIC AND ITS RELATION TO THE HYDROGRAPHY. By Martin W. Johnson. 1956. 32 pages, 15 tables, and 11 figures. *Price: \$0.50.*
- Number 2. THE MAMMALS OF BANKS ISLAND. By T. H. Manning and A. H. Macpherson. 1958. 74 pages, 35 tables, and 15 figures. *Price: to Members of the Institute \$1.00; to non-Members \$2.00.*
- Number 3. THE VEGETATION OF NORTHERN MANITOBA. III. STUDIES IN THE SUBARCTIC. By J. C. Ritchie. 1959. 56 pages, 12 tables, 8 figures, and 8 plates. *Price: to Members of the Institute \$1.00; to non-Members \$2.00.*
- Number 4. THE RELATIONSHIP OF THE PEARY AND BARREN GROUND CARIBOU. By T. H. Manning. 1960. 52 pages, 25 tables, 9 figures. *Price: to Members of the Institute \$1.00; to non-Members \$2.00.*
- Number 5. MARINE INFAUNAL BENTHOS IN ARCTIC NORTH AMERICA. By Derek V. Ellis. 1960. 56 pages, 9 tables, 17 figures, and 2 plates. *Price: to Members of the Institute \$1.00; to non-Members \$2.00.*
- Number 6. THE MEDUSAE OF THE CHUKCHI AND BEAUFORT SEAS OF THE ARCTIC OCEAN INCLUDING THE DESCRIPTION OF A NEW SPECIES OF *Eucodonium* (HYDROZOA: ANTHOMEDUSAE). By Cadet Hand and Lai Bing Kan. 1961. 23 pages, 7 tables, 9 figures. *Price: to Members of the Institute \$0.50; to non-Members \$1.00.*
- Number 7. OBSERVATIONS ON CANADIAN ARCTIC *Larus* GULLS, AND ON THE TAXONOMY OF *L. thayeri* BROOKS. By A. H. Macpherson. 1961. 40 pages, 6 tables, 3 figures, and 6 plates. *Price: to Members of the Institute \$1.00; to non-Members \$2.00.*
- Number 8. THE ARCHAEOLOGY OF THE LOWER AND MIDDLE THELON, NORTHWEST TERRITORIES. By Elmer Harp, Jr. 1961. 74 pages, 15 figures, 12 plates. *Price: to Members of the Institute \$1.00; to non-Members \$2.00.*
- Number 9. A GEOBOTANICAL SURVEY OF NORTHERN MANITOBA. By J. C. Ritchie. 1962. 47 pages, 5 tables, 8 figures, 2 folding maps. *Price: to Members of the Institute \$1.00; to non-Members \$2.00.*
- Number 10. ESKIMO ADMINISTRATION: I. ALASKA. By Diamond Jenness. 1962. 64 pages, 2 figures. *Price: to Members of the Institute \$2.00; to non-Members \$3.00.*
- Number 11. PREHISTORIC CULTURAL RELATIONS BETWEEN THE ARCTIC AND TEMPERATE ZONES OF NORTH AMERICA. Symposium volume edited by John M. Campbell. 1962. 18 papers. 182 pages, 1 table, 7 figures, 34 plates. *Price: to Members of the Institute \$3.00; to non-Members \$4.00.*
- Number 12. THE DYNAMICS OF CONDITION FACTORS IN CANADA GEESE AND THEIR RELATION TO SEASONAL STRESSES. By Harold C. Hanson. 1962. 68 pages, 26 tables, 12 figures, and 7 plates. *Price: to Members of the Institute \$1.00; to non-Members \$2.00.*
- Number 13. RADIOLARIA IN PLANKTON FROM THE ARCTIC DRIFTING STATION T-3, INCLUDING THE DESCRIPTION OF THREE NEW SPECIES. By Kunigunde Hülsemann. 1963. 51 pages, 5 tables, 24 figures. *Price: to Members of the Institute \$1.00; to non-Members \$2.00.*
- Number 14. ESKIMO ADMINISTRATION: II. CANADA. By Diamond Jenness. 1964. 186 pages, 12 figures, folding map. *Price: to Members of the Institute \$3.00; to non-Members \$4.00.*
- Number 15. THE LEMMING CYCLE AT BAKER LAKE, NORTHWEST TERRITORIES, DURING 1959-62. By Charles J. Krebs. 1964. 104 pages, 50 tables, 10 figures. *Price: to Members of the Institute \$1.00; to non-Members \$2.00.*
- Number 16. ESKIMO ADMINISTRATION: III. LABRADOR. By Diamond Jenness. 1965. 94 pages, sketch-map. *Price: to Members of the Institute \$2.00; to non-Members \$3.00.*
- Number 17. THE CHANDALAR KUTCHIN. By Robert A. McKennan. 1965. 156 pages, 2 figures, 26 plates. *Price: to Members of the Institute \$3.00; to non-Members \$4.00.*
- Number 18. PLEISTOCENE GEOLOGY OF ANAKTUVUK PASS, CENTRAL BROOKS RANGE, ALASKA. By Stephen C. Porter. 1966. 100 pages, 22 figures (including folding map), 25 plates. *Price: to Members of the Institute \$2.00; to non-Members \$3.00.*
- Number 19. ESKIMO ADMINISTRATION: IV. GREENLAND. By Diamond Jenness. 1967. 176 pages, 28 tables, 12 figures. *Price: to Members of the Institute \$3.00; to non-Members \$4.00.*
- Number 20. GEOPHYSICAL MEASUREMENTS ON THE KASKAWULSH AND HUBBARD GLACIERS, YUKON TERRITORY. By Garry K. C. Clarke. 1967. 34 pages, 5 tables, 14 figures (including folding map). *Price: to Members of the Institute \$2.00; to non-Members \$3.00.*



PUBLICATIONS COMMITTEE

Chairman: Svenn Orvig, Montreal, P.Q.
Henry B. Collins, Jr., Washington, D.C.
Moir Dunbar, Ottawa, Ont.
Walter Sullivan, New York, N.Y.
Norman J. Wilimovsky, Vancouver, B.C.

CONTRIBUTIONS TO THE *TECHNICAL PAPERS*

Scientific papers on all aspects of arctic work which are either too technical or too long for publication in the Institute's journal *Arctic*, may be submitted for publication in the *Technical Papers*. Manuscripts should be complete with maps, diagrams, and good glossy enlargements of photographs. Proofs will be sent to authors for correction.

An allowance of free reprints will be made.

All manuscripts should be addressed to the Editor, the Arctic Institute, 3458 Redpath Street, Montreal 25, P.Q., Canada.

